Contents lists available at ScienceDirect

Thin-Walled Structures

journal homepage: http://ees.elsevier.com

Residual stresses in cold-formed steel members: Review of measurement methods and numerical modelling

A. Díaz [a,*], I.I. Cuesta [a], J.M. Alegre [a], A.M.P. de Jesus [b], J.M. Manso [c]

[a] Structural Integrity Group, Escuela Politécnica Superior, Universidad de Burgos, Avda. Cantabria S/n, 09006, Burgos, España, Spain
[b] Mechanical Engineering Department, SMPT, Faculty of Engineering, University of Porto, Rua Dr.Roberto Frias, S/n, 4200-465, Porto, Portugal
[c] Sustainable Construction Group, Escuela Politécnica Superior, Universidad de Burgos, Calle Villadiego S/n, 09001, Burgos, España, Spain

ARTICLE INFO

Keywords
Cold forming
Residual stress
Sectioning
Hole drilling
X-ray diffraction
Numerical modelling

ABSTRACT

The determination of residual stress distributions in cold-formed members is revisited considering both experimental and numerical methodologies. Destructive, semi-destructive and non-destructive techniques are reviewed with special emphasis on sectioning, hole drilling and X-ray diffraction; the particularities of each procedure on cold-formed sections are addressed. Theory on metal strip deformation and roll design is exposed before analytical and incremental closed-formed expressions are presented and compared to experimental results for press-braked sections. Finally, the most important works on finite element simulations of roll forming are revisited, highlighting the computational limitations and the capability for predicting residual stresses.

1. Introduction

Manufacturers and engineers require a comprehension of the relationship between manufacturing process, mechanical performance and structural integrity of the corresponding in-service member. The use of different steel sections is common in industry and construction, including lightweight thin-walled sections [1,2] for light steel frames (LSF) and thicker members for conventional building structures [3,4]. Following European Standards, Part 1-1 of Eurocode 3 –EN 1993-1-1: *General rules and rules for buildings*– only covers sections with material thickness greater than 3 mm [3] while Part 1–3 –EN 1993-1-3: *General rules - Supplementary rules for cold-formed members and sheeting*– deals with cold-formed members [5]. Roll forming is also an economic alternative for the automotive industry [6,7].

Forming processes in metallurgy are characterised by a deformation beyond the elastic range with the aim of a permanent effect in shaping operations, so a plastic deformation is involved. In the context of material science and mechanics, plasticity mechanisms and modelling are still an open research field [8,9]; besides, due to the non-linearity of plastic processes, the associated computational problem is also a complex issue [10,11]. Deformation history during forming influences thus the mechanical behaviour of members in structural systems [12–14]. However, a distinction between cold and hot forming is useful to decide if deformation history is critical. Hot forming processes are carried out above the recrystallization temperature of the metal so the deformation-induced phenomena are mitigated [15] and, thus, residual stresses are mainly created by non-uniform cooling [16]. In contrast, cold forming processes are obviously associated to an important cold working since the deformation is performed below the recrystallization temperature [16], which is usually considered around 590 to 760 °C for steels, particularly 727 °C for low carbon steels [17].

Cold working involves hardening due to the generation of dislocations [18] but also a likely ductility reduction [19]. Grain structures are also modified during cold rolling due to the elongation in forming direction [20] and the formation of sub-grains and cell blocks because the dislocation multiplication [21,22], giving place to anisotropic mechanical properties of the finished formed member, especially for high thickness reduction levels [23]; this strengthening effect induced by cold rolling is usually applied to TWIP (Twinning-Induced Plasticity) steels [24]. Phase transformation is also possible during cold working of austenitic stainless steels where deformation can induce martensite transformation [25]. All of these microstructural changes promote a crystal distortion that induces residual stresses at both micro and macro scales [26].

Steel is more pliable at high temperatures and residual stresses are avoided but hot forming has some limitations in geometric tolerances [27,28] and in thicknesses [29]. Due to the fast cooling of thin sheets, the minimum thickness that can be reached through hot rolling is about 1.5–1.8 mm [17]. Additionally, the process can be expensive due to the cost associated to energy input for heating [30]. Many times, hot and cold rolling processes are combined so to reduce the metal slab thickness in two steps [17]. For instances, the mother coils that are

* Corresponding author.
E-mail address: adportugal@ubu.es (A. Díaz)

https://doi.org/10.1016/j.tws.2020.107335
Received 22 May 2020; Received in revised form 10 November 2020; Accepted 24 November 2020
Available online xxx
0263-8231/

then cold-formed, through cold roll forming or through press braking, could have been produced by hot rolling.

The present review is focused on cold forming in two variants: roll forming (RF) and press braking (PB). This work aims at gathering and critically discussing the state of the art of residual stress determination in thin-walled steel sections that have been manufactured by cold forming processes. As shown in Fig. 1, press braking is based on consecutive bends of a metal sheet that is forced by a punch towards a die, so a corner is formed. On the contrary, during roll forming a flat sheet is progressively folded due to the action of rolls or mills that are separated by a certain distance. Therefore, deformation mechanisms during roll forming and press braking are substantially different even if the same shape was obtained. Industrial production of complex sections is expected to be slower using press braking than roll forming, so the latter is being preferred to reduce costs and times [31,32]. Press braking can be competitive for short runs or simple section geometries [33]. However, roll forming requires a more careful tool design and installation [32]. A comprehensive review of roll forming as a manufacturing process, i.e. equipment, process parameters, tool design, practice, troubleshooting, etc, is not the aim of this paper. For this information, the Roll Forming Handbook by Halmos is suggested to the reader [17].

Section design is based on loading conditions and members can be divided in compression and flexural members. Additionally, since cold-formed members are usually thinner in comparison to hot-rolled sections, the compression failures modes to be considered are generally more complex, including local and post-buckling phenomena [36]. Residual stresses affect structural performance of steel members both for instability failures [37–39] and for fracture and fatigue near stress concentrators [40–42]. Especially for fatigue, residual stress levels at welded joints are expected to affect the service life of structures [43]. It must be noted that Eurocode 3 EN-1993, part 1–9 [44], only covers hot-rolled steel details and there is a lack in design and fatigue assessment rules for cold-formed sections at European level. AISI design guides have been developed for cold-formed steel sections by LaBoube and Yu [45], mainly based on a review of available test data [46,47]. Within this context, structures can suffer unexpected fracture failures even within the design load range due to the presence of cracks, which appear because of deficient welding, corrosion phenomena or fatigue [36]. Research on connection design and failure is reviewed by Lee et al. [48] for cold-formed sections. Cold forming will influence crack propagation and unstable fracture mainly through two aspects: first, cold working induces hardening and so ductility is expected to be reduced; second, tensile residual stresses will accelerate cracking whereas cracks can be arrested in compressive regions. Thus, residual stress distributions should be mapped for a certain manufacturing process and related to the forming parameters. However, due to relatively infrequent use of a fracture mechanics approach for cold-formed structures, residual stresses are taken into account generally only to avoid geometrical consequences, e.g. curving, bow section or deviation from flatness [17].

The average design strength is also affected by residual stresses so cold forming influence can be introduced following the formula provided by Eurocode 3 Part 1.3 that takes into account the forming process and the number of 90° bends of the section [49]. Additionally, Eurocode considers that for hollow sections the cold-formed members must be designed considering a more restrictive buckling curve in comparison to hot finished sections [5]. The higher imperfection factor for cold-formed sections includes geometrical and mechanical imperfections, i.e. the likely presence of residual stresses [50].

Prediction of residual stresses must rely on a robust experimental-numerical framework. However, the complex manufacturing processes, especially roll forming, difficult generalised distributions [51,52]. The intersection between academy and industry is also problematic: simplification and idealisation of real manufacturing processes could hide from view the daily procedures that introduce uncertainties, non-reproducibility and scatter between samples [53,54]. Additionally, the influence of secondary processes, e.g. coiling, storage and transport, can surpass forming effects on residual stresses [17,55,56].

The objective of this work is to review the existent procedures to assess residual stresses in cold-formed steel members, both numerically and experimentally. In section 2, methods for residual stress measuring are reviewed following the usual classification into destructive, semi-destructive and non-destructive techniques. Special emphasis is put on sectioning, hole drilling and X-ray diffraction methods, since these are widespread procedures. Particularities of measurements on cold-formed thin-walled steel members are exposed, addressing the applicability, range and limitations of each method. Numerical modelling of residual stresses due to cold forming is treated in section 3. First, the common mathematical procedures to optimise roll design are revisited following strip deformation theories. Then, residual stress predictions based on analytical assumptions are exposed as well as the computational framework for finite element simulations of forming processes.

2. Measurement methods

The most common classification of methods for residual stress determination is based on the destructivity of the measurement. Rossini et al. [57] cited the principal techniques among destructive, semi-destructive and non-destructive, as shown in Fig. 2 in which methods are also classified according to the underlying physical principle: relaxation, diffraction or other phenomena [58].

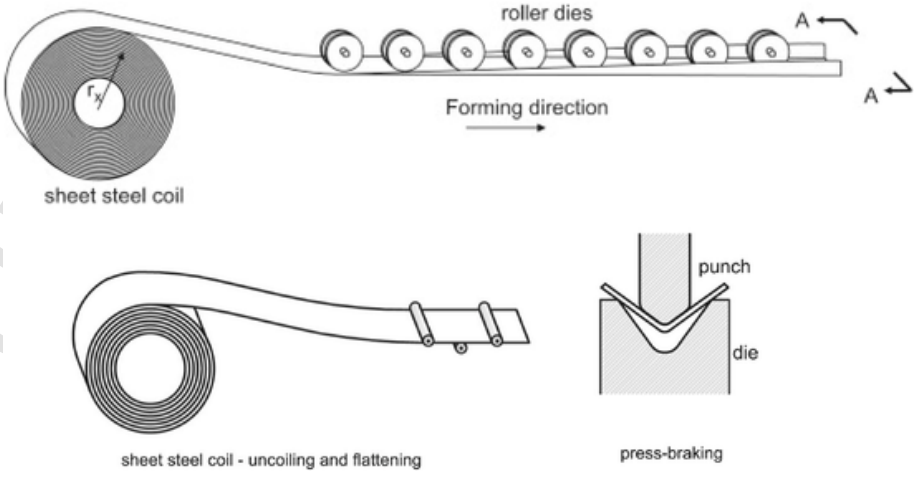

Fig. 1. Comparison of roll forming (top) and press braking (bottom) from a sheet steel coil [34,35].

	Destructive	Semi-destructive	Non-destructive
Relaxation	▪ Sectioning ▪ Contour	▪ Hole drilling ▪ Ring core ▪ Deep hole drilling	
Diffraction			▪ X-ray diffraction ▪ Neutron diffraction
Other principle			▪ Ultrasonic ▪ Magnetic Barkhausen noise

Fig. 2. Classification of common residual stress measuring methods [57,58].

The present section references are not limited to cold-formed profiles but refers to (i) general considerations of measurement methods and (ii) residual stress determination in steel members that share the same purposes and limitations for measurement: thin walls, stress concentrators near bent corners (and sometimes welds) and inner surfaces that can be hardly accessible. Thus, studies on steel sections produced by other manufacturing process, e.g. hot rolling or extrusion are also considered in this section. Works studying cold-rolled plates in which the rolling process is aimed at thickness reduction and work hardening rather than the section shaping are also included.

Some authors have combined different destructive, semi-destructive and non-destructive techniques to analyse residual stresses in cold-formed steel samples. Roy et al. [59] (1994) studied cold-formed steel sections using techniques over the whole classification range, as shown in Fig. 2: hole drilling, X-ray diffraction, slicing and magnetic (Barkhausen noise) methods. Bouffioux et al. (2016) [60] compared X-ray diffraction, ring core and sectioning methods for the analysis of residual stresses in hot-rolled sheet piles that have been straightened through a rolling process.

The combination of different techniques is a common practice to assess possible bias and to exploit the advantages of each method. However, this approach is not always available, and the analysis of steel members are focused on a specific technique. The next sections gather and review literature using different methods for determining residual stresses. Residual stresses could also be indirectly related to hardening phenomena trough different experimental procedures, e.g. local tests for the determination of stress enhancement due to cold forming [32] or micro-hardness measurements [61]. However, stress enhancement measurement is out of the scope of the present work but it is addressed elsewhere [32,62].

2.1. Destructive methods: sectioning

Sectioning method is a denomination that comprises cutting methods that can be used to qualitatively [63] or quantitatively [64] analyse the altered geometry after cutting due to the release of the locked-in residual stresses. Strip cutting is carried out in some works using mechanical saws [65] (refer to Fig. 3) but it is recommended to substitute these rough operations by more refined cutting methods, e.g. wire-cutting [66,67], electro-discharge machining (EDM) [68] or spark erosion layering [37], in order to reduce vibrations, heating and strain gauge damage. For longitudinal members, i.e. where axial dimension is high in comparison to the cross section, two sectioning strategies can be followed:

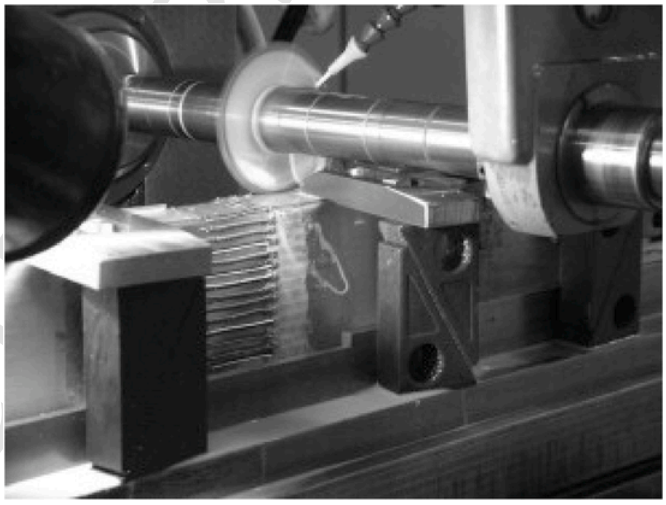

Fig. 3. Sectioning of a cold-rolled stainless steel box section [26].

- **Longitudinal sectioning:** strips are mechanically cut along the axial direction so longitudinal stresses are obtained.
- **Transversal sectioning:** cutting operation is performed in a direction parallel to the cross section so transversal stresses are determined.

The longitudinal cutting is more common for cold-formed steel members since longitudinal stresses are expected to influence buckling performance [69]. However, transversal stresses can be critical for mechanical resistance, including fracture and fatigue behaviour near stress concentrators [70]. The cutting pattern that can be found in the work of Quach and Young (2015) [67] for elliptical hollow sections (EHS), considering 48 longitudinal strips and 20 transversal measurements, both in inner and outer surfaces, is representative of the sectioning capabilities. Ueda et al. [71–73] proposed an analytical-experimental methodology to determine three-dimensional strain distributions based on sectioning and different slicing strategies and introducing the concept of inherent strains. This procedure, also named as eigenstrain method, was proposed for welded joints and has been revisited by Hill et al. [74,75] but its use has not been generalised and longitudinal sectioning is the preferential choice.

Deformation of strips after relieving can be interpreted visually to assess the existence of stresses and to determine its sign. As shown in Fig. 4, residual stresses are usually linearized considering that the dis-

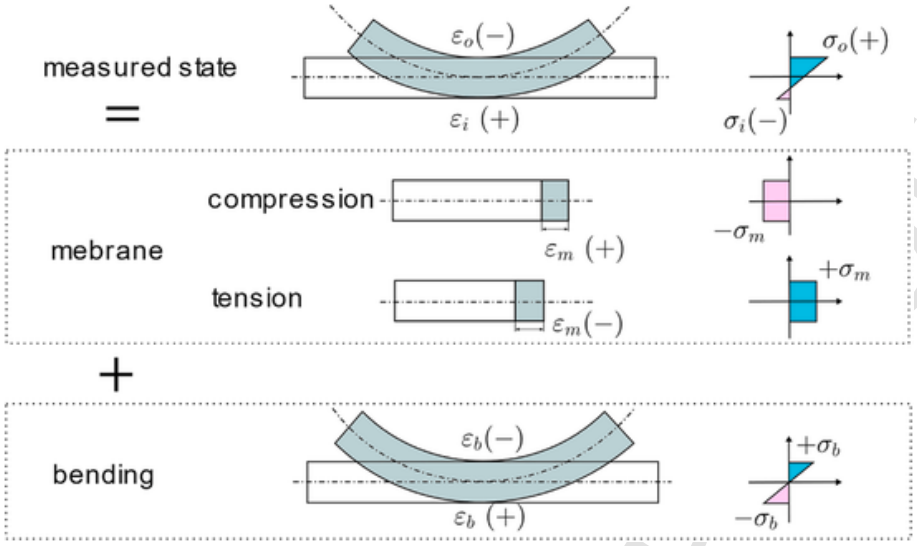

Fig. 4. Linear assumptions of residual stress distributions: membrane and bending components [66].

tribution through thickness can be decomposed into membrane and bending stresses [66]. After cutting, the relieve of pre-existing tensile residual stresses will produce the shrinkage of the corresponding fibre, whereas compressive stresses relieve will cause its lengthening. Linear assumptions will be critically revisited in Sections 3.2 and 3.3 where it is demonstrated that this simplification can highly deviate from distributions numerically obtained.

Due to the wide range of commercial strain gauges and the ease of installation, this method is simple and economical. However, strain gauge positioning is complex on hardly accessible surfaces; gauges should also be protected [76] from contamination by cutting debris and lubricating products. Due to the heat generation during sectioning, which depends on the cutting procedure as mentioned above, coolant products are sometimes used, so the protection of strain gauges by waterproof glues can be considered [67]. Deviations from unstrained electric resistance are automatically translated by data acquisition modules, taking into account the gauge factor provided by the supplier, to strain measurements. Stress determination assumes elastic proportionality between residual stress and the strain measured on the surface of the sectioned strip. Outer and inner stresses (σ_o and σ_i) are simply determined by the following Hooke's law:

$$\sigma_o = -E\varepsilon_o \# \tag{1}$$

$$\sigma_i = -E\varepsilon_i \# \tag{2}$$

where ε_o and ε_i are the measured relieved strains on the outer and inner surfaces, respectively. Assuming the linear decomposition, residual stresses can be expressed through membrane, σ_m, or bending, σ_b, components [66]:

$$\sigma_m = -E\frac{\varepsilon_o + \varepsilon_i}{2} \# \tag{3}$$

$$\sigma_b = \pm E\frac{\varepsilon_o - \varepsilon_i}{2} \# \tag{4}$$

These expressions are valid for pure elastic unloading. Reverse yielding during stress relieve and cutting-induced plasticity phenomena are usually neglected in sectioning. However, the latter can reduce accuracy of contour methods for determining residual stresses [77–79]. It is important to recall the implications of the sectioning procedure on the stress measurement scale: this method determines the averaged stress value for the whole strip width [80]. Hence, comparison with other local techniques, e.g. hole drilling or X-ray diffraction, is not easy.

Dat and Pekoz (1980) [81] measured residual strains for press-braked and roll-formed steel hat channels. For both cold forming processes the authors found tensile residual stresses on the outer surface of the channel and compressive in the inner surface along the longitudinal direction. The relieved strains due to the strip cutting were higher near corners in comparison to the flat parts. A similar approach was followed by Weng and Pekoz (1990) [82] but they showed that Electro Discharge Machining method is a better alternative than saw cutting for residual stress measurement by sectioning. Key and Hancock (1993) [37] used the sectioning method for the determination of surface longitudinal stresses on a roll-formed Square Hollow Section (SHS) whereas the distribution through the thickness was measured using a spark erosion layering technique which is based on the material removal of small blocks extracted from the member. This approach gives a more detailed through-thickness stress distribution, as shown in Fig. 5 for a SHS of 254 × 254-mm^2 section, 6.3 mm of thickness and 405 MPa of yield stress. It can also be concluded that linearization oversimplifies the real zig-zag distribution.

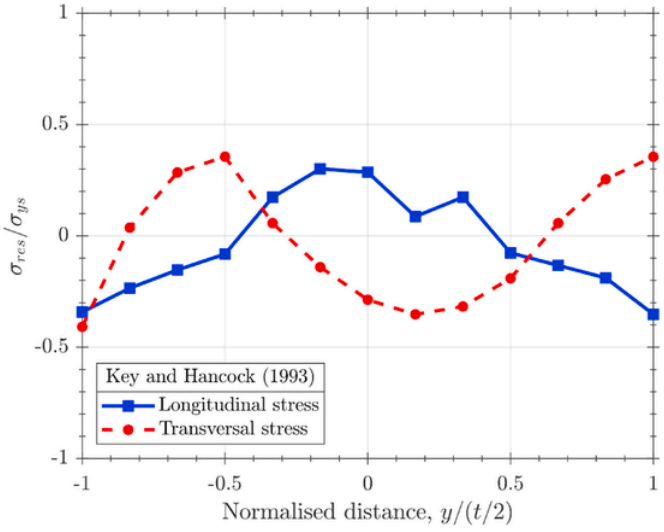

Fig. 5. Residual stress distribution through the thickness of a cold-formed SHS using a layering method [37].

Ingvarsson (1975) [83] also used the sectioning method for the determination of residual stresses in a press-braked U-section. Batista and Rodrigues (1992) [84] compared press-braked and roll-formed C-shaped sections using the strip sectioning method and stated that longitudinal stresses are higher for the roll-formed profiles than for the press-braked sections. For both members the membrane stresses were very low.

Schafer and Pekoz (1998) [51] collected longitudinal residual stresses from the previously cited works [37,81,83–87] that used sectioning techniques and represented statistical averages for 16 press-braked and 13 roll-formed steel members, as shown in Fig. 6 for the bending residual stresses; as already mentioned, the membrane stresses were found to be very small. However, other authors [88,89] have found for press-braked lipped channels that bending residual stresses are even lower (less than 7% of the yield stress) so they can be neglected in the subsequent structural analysis [90,91].

This comparison between manufacturing procedures, roll forming and press braking, was also carried out by Cruise and Gardner (2008) [26] for stainless steel box sections using the sectioning technique. They confirmed that longitudinal residual stresses are higher for roll forming [26]. Cold-formed angle columns produced by press braking were studied by Ellobody and Young [92] using sectioning by wire-cutting. In that work, recorded strains were corrected for temperature effects. They found, in contrast to the results cited above, that longitudinal residual stresses are negative in the outer surface of corners, i.e. the stresses are not uniform and shift to compression on the bent regions. Those results were confirmed for other press-braked double lipped samples [93]. In both works the membrane stresses were not negligible and reached about 50–100 MPa at corners.

Ma et al. (2015) [66] investigated high strength steels hollow sections with different section shapes: circular, square and rectangular. Sectioning technique was not only performed in longitudinal strips but also through cutting transverse rings. The measured membrane and transverse stresses were not negligible; these results are also supported by the measured changes in corner angles of sectioned rings. Somodi and Kövesdi (2017) [94] measured longitudinal residual stresses on high strength steel SHSs produced by continuous cold forming. The sectioning method was used in that work. These authors also reviewed literature on residual stress determination on cold-formed SHSs.

Law and Gardner (2012) [95] applied the sectioning technique to assess residual stress effects on lateral instability of elliptical hollow steel sections (EHS) that were hot-finished, finding residual stress magnitudes about 10–15% of the yield stress and negligible influence on structural response. The compressive and tensile residual stresses in inner and outer surfaces, respectively, found by Law and Gardner (2012) [95] were confirmed in EHS by Quach and Young (2015) [67]. Analysing results from Law and Gardner (2012) [95] and those from Quach and Young (2015) [67], it might be concluded that for the same section the heat treatment has a critical influence; however, direct comparison between different manufacturing processes is problematic because Quach and Young (2015) [67] detailed the rolling operations but little information is given in Ref. [95]. Quach and Young (2015) [67] also demonstrated that, as expected, cold-rolled EHSs present much higher residual stresses in comparison to hot-finished specimens.

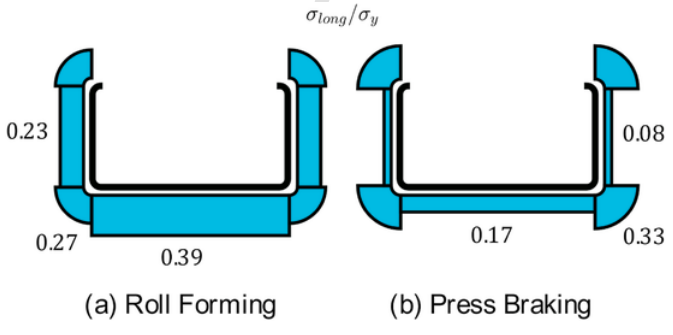

Fig. 6. Bending residual stresses in longitudinal direction, collected by Schafer and Pekoz (1998) [51].

2.2. Semi-destructive methods: hole drilling

Some techniques to determine residual stresses are based on measuring strain relieve during drilling operations on a target material. Three methods are here reviewed:

- **Hole drilling method (HD):** this is the most common method and it is based on incrementally drilling and registering of the relieved strains around the hole. It is usually named as incremental hole drilling (IHD) to avoid confusions with deep hole drilling or as centre-hole method to differentiate it from ring core method.
- **Ring core method (RC):** the procedure relies on the same principle, but the drilling tool is an annular cutter, and the strain gauge rosette is placed within the removed ring.
- **Deep hole drilling method (DHD):** this is a more complex technique in which a long hole is performed using a gun-drill and the reference diameter is measured with an air probe; then, a cylinder containing the hole is trepanned and, finally, the diameter of the reference hole is measured again [96,97].

DHD is used for workpieces with a minimum thickness of 6 mm [98] but is optimally applied to metal thick plates and sleeves [99] since the advantage over other techniques is palpable for great depths, from 10 to 100 mm [96]. Even though strain sensitivity of RC and HD methods limits the maximum measured thickness [99], for thin-walled cold-formed sections, HD and RC are preferred due to its simplicity.

As shown in Fig. 7, RC method requires strain gauge rosettes with overlapping measuring grids [100]. It is less common than hole drilling and is not standardised [101]. However, non-uniform residual stress calculation from the strain registered during ring core milling is also based on the integral method, which is used in the hole drilling procedure [100] Calibration matrices are also found through Finite Element simulations for the corresponding geometry [102,103]. Both hole drilling (HD) and ring core (RC) methods can be performed at a micro-scale using advanced techniques as Focused Ion Beam to drill holes [104,105] or remove annular trenches [105–107] and to determine micro-residual stresses in thin films or coatings. Strain relief thus must be registered using Digital Image Correlation (DIC) [104,106] instead of strain gauge rosettes.

Since more material is removed in RC method, the strain error accumulation and the corresponding stress uncertainty is avoided in comparison to HD [101]. However, ring core is thus more destructive and the measurement scale is larger – the milled ring has usually inner and outer diameters of 14 and 18 mm, respectively, and the hole depth reached 5 mm [100,103] – so these advantages are only justified for thick workpieces or when residual stress distributions are searched over a relatively large area. Regarding the study of cold forming influence on residual stresses, thin members need to be analysed so hole drilling is the preferred method. This subsection is hereafter focused on the incremental hole drilling method as described by the ASTM E837-13a Standard [108].

The determination of in-depth residual stresses using the hole drilling method can be divided in three stages:

1. Drilling a hole incrementally, i.e. dividing the total depth in steps. Usually, 1 mm of hole depth is divided in 20 steps of 0.05 mm.
2. Measuring relieved strains after each drilling step. Different strain gauge rosettes models are used to register micro-strains, but the typ-

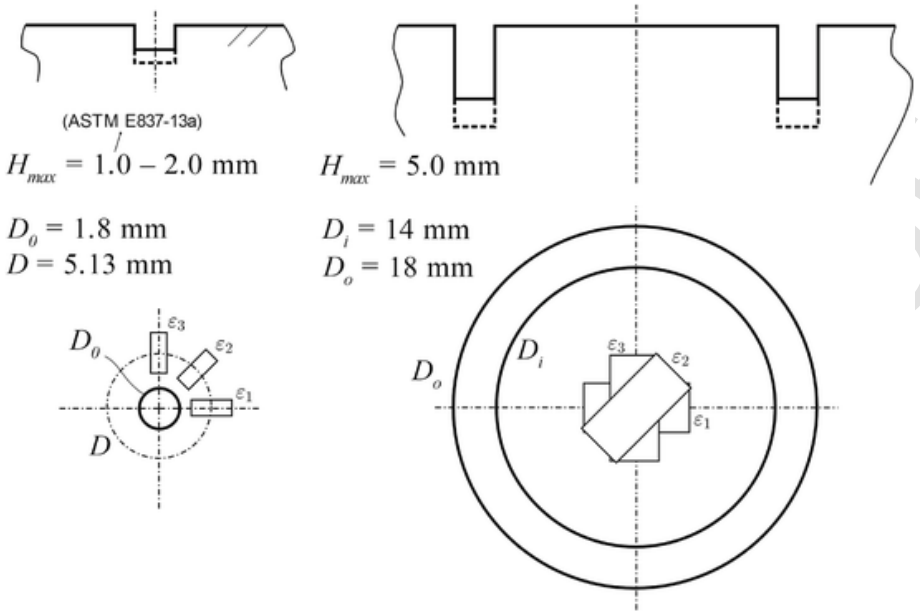

Fig. 7. Typical dimensions of hole drilling versus ring core procedures; adapted from Ref. [100].

ical Type A and B consist of three grids and are defined in the ASTM E837-13a Standard.

3. After the experimental stages 1 and 2, the three strain distributions that have been registered in each grid are used to determine residual stresses. The most common algorithm to solve the associated inverse mathematical problem is the integral method in which a matrix system is solved using calibration coefficients that are defined in the ASTM E837-13a Standard for the generic situation or can be found through Finite Element calculations [109].

One advantage of this procedure lies in the determination of three stress components in only a single drilled hole; thus, the complete stress state is described. In contrast, XRD requires a tilting sequence for each direction [60]. Additionally, layer removal is inherent to the method and surface electropolishing is not required for the determination of in-depth distributions when the non-uniform stress determination is considered following ASTM E837-13a. However, the strain gauges are less sensitive to the stress removal of deep layers, so the Hole Drilling procedure is usually limited to 1 mm for holes of approximately 2 mm of diameter [108].

The matrices of calibration coefficients included in the ASTM E837-13a Standard have been calculated for a thick target workpiece and for a hole diameter $D_0 = 2$ mm. This fact can limit the applicability of the hole drilling method. Actually, the ASTM E837-13a standard is limited for the analysis of thin pieces considering uniform stresses and for thick pieces for non-uniform stress distributions. The range of allowed thicknesses is relative to the diameters of the hole (D_0) and the strain gauge rosette (D). For the most common strain gauge rosettes, i.e. $D = 5.13$ mm, the analysed workpiece must be thicker than 5.13 mm for the determination of non-uniform residual stresses while for plates thinner than 1.03 mm the ASTM E837-13a Standard allows the calculation of uniform stresses [108]. Regarding the hole diameter, the standards gives matrices for $D_0 = 2$ mm and proposes a correction expression, as long as D_0 lies between 1.88 and 2.12 mm for the common rosettes ($D = 5.13$ mm). Alegre et al. (2019) [110] have demonstrated that deviations from this correction can be critical for very small holes. However, the commercial drill bits and strain gauge rosettes are usually designed considering holes between 1.6 and 2 mm of diameter. The main optical alternatives to the use of strain gauges during hole drilling are holographic interferometry [111,112], moiré interferometry [113,114], electronic speckle pattern interferometry (ESPI) [115–117] and digital image correlation (DIC) [118,119]. It must be noted that hole drilling method usually assumes a biaxial state ($\sigma_z = 0$) due to the proximity to surface and only in-plane stresses are considered within the integral method [120]. Some authors have added a displacement transducer in the drilling direction to determine the triaxial residual stress state both for hole drilling and ring core methods [121].

All methods based on material removal and measurement of stress relieve assume elastic unloading [97]. This assumption is not valid for residual stresses whose magnitude is close to the yield limit because, during relaxation, the drilled hole acts as a stress concentrator and the unloading process can produce plasticity around it [122]. For DHD, Mahmoudi et al. (2008) [97] have introduced corrections to elastic solutions in order to measure residual stresses near the yield stress magnitude. Ring core elastic solutions have been also modified by some authors with the aim of including plasticity effects [123,124]. However, more research has dealt with plasticity corrections for the hole drilling method. Yan et al. (1996) [125] proposed a numerical methodology to correct residual stresses considering calibration coefficients that depend on the distortion energy. Vangi and Ermini (2000) [126] improved this approach by considering the effect of biaxiality and the orientation of strain gauges with respect to the principal directions. These authors showed that elastic predictions are totally accurate only for stresses lower than the 50% of the yield stress. Beghini et al. [127–131] have also performed an extensive work in quantifying errors associated to plasticity and improving corrections strategies. However, these correction procedures are limited to the determination of uniform distributions. For non-uniform residual stress determination, the inverse problem associated to hole drilling becomes even more complex when plasticity effects are considered. Hence, only equi-biaxial stress states, as those usually produced by shoot peening, have been considered for plasticity corrections and non-uniform in-depth distributions [132]. Artificial neural networks have been successfully applied to solve the inverse problem of plasticity correction in peened surfaces [133]. However, the equi-biaxial simplification is hardly applicable to cold-formed members.

Following the mentioned works it is well established that the ASTM E837-13a Standard overestimates residual stresses in the near-yield stress range and only predicts “satisfactory” results when residual stresses do not exceed the 80% of the yield stress in a thick workpiece

and the 50% of the yield stress in a thin workpiece [108]. As shown in Fig. 6, considering the sectioning results collected by Schafer and Pekoz (1998) [51], residual stresses are expected to be lower than the 50% of the yield stresses. On the other hand, the mentioned thickness range covered by the ASTM E837-13a Standard limits the applicability of hole drilling non-uniform stress algorithms for thin workpieces, which is extremely important within the context of thin-walled steel members manufactured by cold forming. Thus, much effort is being put on the extension of the procedure to intermediate thicknesses [110,134]. Calibration coefficients have been included in a compact polynomial formulation by Schajer (2020) [135]. As shown in Fig. 8, the calibration coefficients forming the matrix $\bar{a}_{jk}$ for non-uniform stress determination can be recalculated for "thin" workpieces [110]; in this case, results for 1.5-mm thickness have been obtained by Alegre et al. (2019) [110]. The authors also studied the influence of a round surface near the drilled hole on the relieved strains and the corresponding calculated stresses [136].

For thin cold-formed specimens, two approaches are feasible: (i) the non-uniform determination of residual stresses up to the depth limited by the strain gauge sensitivity; (ii) the uniform determination of residual stresses and a possible subsequent layering of the thickness. Using the first strategy, only the 1-mm in-depth distribution is determined with the most common rosettes and hole diameters, but with the latter, i.e. layer removal, the advantage of hole drilling versus X-ray diffraction is pointless.

2.2.1. Non-uniform stress determination

Schuster et al. (2017) [137] studied plastic corrections, including anisotropy, for Hole-Drilling calculations in thin cold-rolled specimens of a dual phase DP600 steel. The novelty of their work lies in the simultaneous consideration of plasticity and thickness effects.

De Giorgi (2011) [138] studied residual stresses in cold-rolled steel plates using the hole drilling method and a correlation between micro-hardness values and local yield strengths so the cold work level due to the rolling reduction process might be evaluated. A total depth of 2 mm was analysed. It must be noted that for analysis beyond the 1-mm depth limit for $D = 5.13$ mm two options are possible: the use of larger rosettes or the consideration of the HD method proposed by the University of Pisa in which generalised influence functions are analytically defined [139–141].

Non-uniform stress determination was also carried out by Lothhammer et al. (2017) [117] for cold-formed tubular sections using the hole drilling method combined with Digital Speckle Pattern Interferometry (DSPI) instead of strain gauge rosettes. They compared two forming process: (i) UOE, which stands for a combination of pressing steps: U-shaping (U), O-shaping (O), edge welding and a final expansion (E). (ii) a continuous rolling from flat to tubular shape with a continuous electric resistance welding (ERW). In that work, tube wall thicknesses ranged from 10 to 20 mm so the non-uniform stress calculation was allowed without thickness correction.

2.2.2. Uniform stress determination

Weng and White (1990) [64] studied press-braked steel corners using hole drilling and sectioning. They compared both methods and found good agreement. Hole drilling was performed by layering the analysed sections of 25.4 and 38.1 mm of thickness. That study on cold-bent corners demonstrated the influence of bending angle, radius and thickness. As shown in Fig. 9, for a corner of 90° with a thickness of 25.4 mm, the lower R/t ratio produces the higher tensile residual stress value that is found in the inner surface of the corner (92% of yield stress).

Tong et al. (2012) [142] measured roll-formed steel SHS using the hole drilling and the X-ray diffraction methods. The thickness of the section was divided in 4 layers and hole drilling measurements were performed considering the uniform residual stress solution [108] after the corresponding layer removal. In this case, both methods (XRD and HD) require the correction due to relaxation. Zhang et al. (2016) [63] compared residual stresses in hot-rolled and cold-rolled SHSs, as well as heat-treated specimens after cold rolling. As expected, the cold-rolled members showed higher residual stresses. Longitudinal stresses at the outer surface were found to be very high, about 20–30% of the yield stress near corners and up to 60–80% at the middle of the flat area. However, transversal stresses were lower and reached compression values compressive near corners. Hole drilling was used in that work considering the uniform stress procedure but without a following layering, so the results shown in Fig. 10 correspond to the average stresses within the 1-mm surface layer.

Wang et al. (2012) [80] also combined sectioning and hole drilling techniques to analyse longitudinal residual stresses in a high strength steel square section; surface uniform stresses were assumed and no layering was performed. However, the section was formed by welding plates so residual stresses are not comparable to those produced during cold forming.

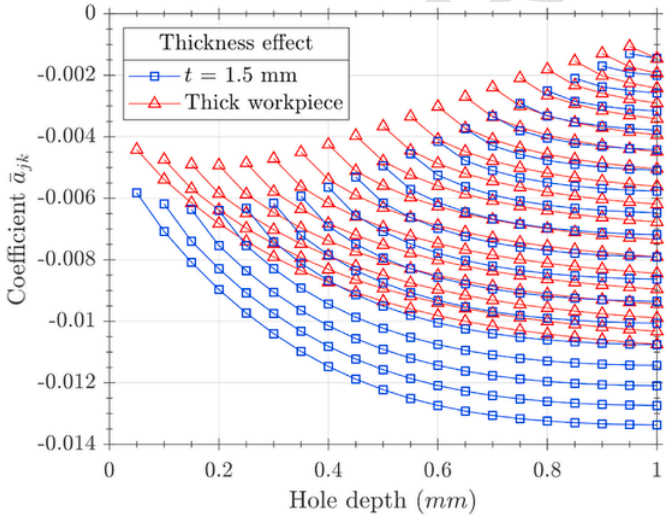

Fig. 8. Coefficients $\bar{a}_{jk}$ calculated through FE simulations for a thickness of 1.5 mm [110] compared to the solution corresponding to a thick piece given by the ASTM E837-13a Standard.

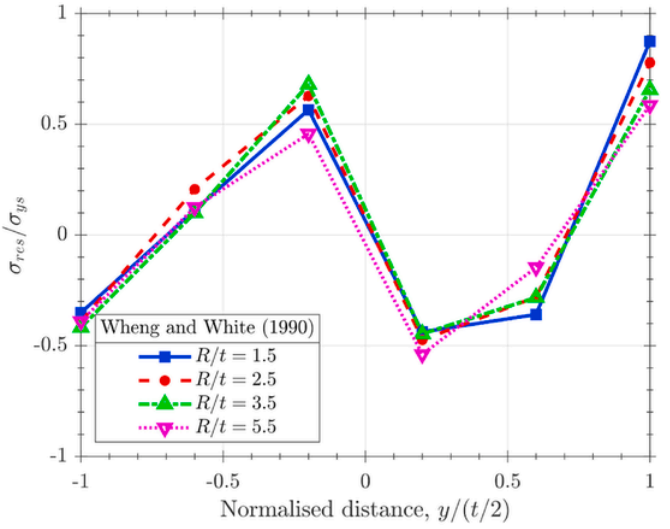

Fig. 9. Transversal residual stresses tangential to a 90° corner in a cold-bent sample of 25.4 mm of thickness. Results extracted from Weng and White (1990) [64].

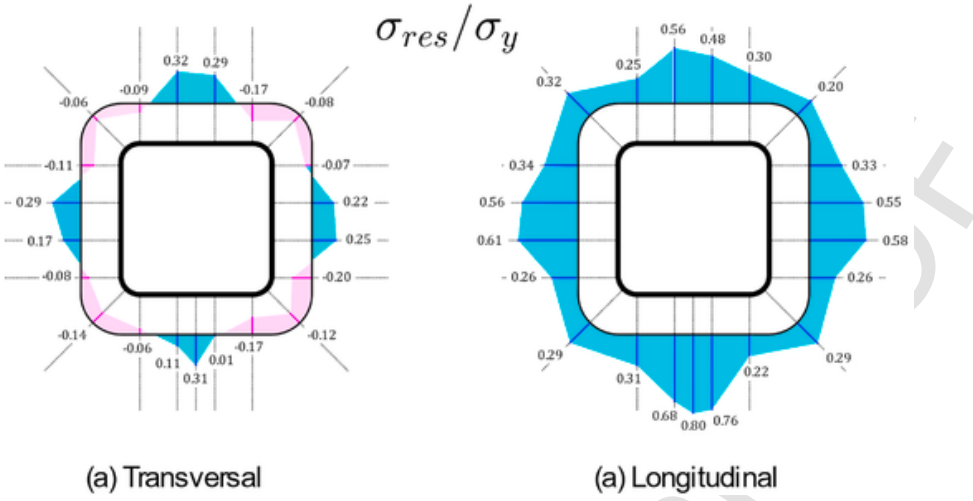

Fig. 10. Residual stresses on the outer surface for cold-formed SHSs extracted from Zhang et al. (2016) [63].

2.3. Non-destructive methods: X-ray diffraction

Destructiveness of the method is not critical within the context of Cold Forming; due to the relatively economic manufacturing process, steel members can be produced only for measurement purposes. In-service residual stress analysis is not required. However, diffraction methods are sometimes employed for two reasons: (i) the expected precision in the determined residual stresses [143] and, (ii) the localised character of measurements, that depends on the collimator diameter: 2 mm in Refs. [60], 1.8 mm in Ref. [144] and 1 mm in Ref. [145]. Nevertheless, a similar scale is obtained using the hole drilling method, following ASTM E837-13a, where a hole of 1.8-mm diameter is usually drilled.

Even though residual stresses found by XRD are considered as surface stresses, diffraction occurs over a finite number of atomic layers; Bouffioux et al. (2016) [60] measured stresses on a hot-rolled sheet for an averaged thickness of 10 μm. Jandera et al. (2008) [144] also assumed that stresses at surface correspond to a depth of 5–10 μm. In that work (refer to Fig. 11), compressive stresses are along the perimeter of the box section both for longitudinal and transversal stresses, in contrast to previous works, as shown in Fig. 6 [51] and 10 [63], where tension stresses were determined. Thus, they also analysed in-depth stresses for three different distances from surface (0.1, 0.3 and 0.5 × thickness) through electrolytical layer removal, finding a through-thickness rectangular block of residual tension which is critical for the buckling response [144]. Wang et al. (2020) [146] measured by XRD only surface residual stresses due to roll forming with the purpose of validation the numerical model; once validated along the section perimeter, the complete through-thickness stress state was assumed to follow FE results. This experimental-numerical approach is pertinent for cold-formed sections to reduce the cost of test and to predict stresses in hardly accessible surfaces.

Other authors have also used XRD to measure residual stresses due to cold-rolling reduction [147–149]. In these cases where plastic straining and thickness reduction are the governing processes, phase transformation and texture evolution can be also analysed through diffraction techniques [148,150]. Within this context, neutron diffraction is a common alternative [151,152] due to its advantage over XRD of greater penetration [153]. Residual stresses through a depth order of centimetres can be measured using neutron diffraction without the need of layer removal [154]. However, this technique is more expensive and, to our knowledge, has not been used for cold-formed steel members. The present review focuses on forming and shaping proce-

Fig. 11. X-ray diffraction apparatus for the residual stress determination in cold-rolled stainless steel hollow sections. Left picture extracted from Jandera et al. (2008) [144]; right picture from Tong et al. (2012) [142].

dures in which plastic straining is only associated to corner bending so texture studies and strain pole figures are not addressed.

For the determination of residual stress through the thickness of a thin sample, material layers are commonly removed by electropolishing. Abvabi (2014) [155] use the XRD method with electropolishing to remove layers of 50 μm. This is equal to the usual step for the hole drilling method. While mechanical removal methods, e.g. electro-discharge machining (EDM), are shown to produce high residual stresses [156], the electrolytical methods as electropolishing do not alter the stress state. The ASTM E1558 – 09 (2014) Standard [157] establishes the recommended procedure for electropolishing without introducing additional residual stresses. However, two phenomena should be considered:

- **Surface damage.** When an excessive potential or polishing time are applied, pitting problems can appear [158]. A careful sample preparation must be done and the selection of electrolytes, potentials and polishing conditions has to be performed following the recommendations from guides and standards [157,159].
- **Relaxation.** For thin members, the layer removal creates relaxation so the measured stresses must be corrected assuming equilibrium conditions [145]. This correction was firstly proposed by Moore and Evans [160] and improved by Savaria et al. [161] using a Finite Element methodology.

As previously mentioned, Tong et al. (2012) [142] measured cold-formed SHSs through hole drilling and X-ray diffraction methods (refer to Fig. 11). The required layer removal was also corrected using elastic expressions considering relaxation. They compared "direct" forming process, in which the SHS is rolled directly from a flat steel plate, with "indirect" or continuous process where a circular section is firstly formed and then rolled to the final square section. Results in the outer surface, as shown in Fig. 12, i.e. $y = -t/2$, correspond to tension longitudinal stresses.

The evaluation of the diffraction intensity curve is usually automatized and only the residual stress is extracted from the $\sin^2\psi$ fitting slope; this fitting method requires a range of tilt angles – 13 tilts in Ref. [60] – in order to find residual stress value for each analysed direction. However, some inner surfaces near bent corners can difficult the goniometer tilting. It must be highlighted that the extent of the diffraction curve, which is quantified by the Full Width at Half Maximum (FWHM), is an interesting parameter for measuring crystal distortion so plastic deformation can be correlated with this value [162,163]. Even though the quantification of plastic deformation can help to improve the understanding of cold forming effects, the study of FWHM parameter is rare in literature about XRD method on cold-formed steel sections [70].

3. Residual stress modelling

Mathematical modelling, both analytical and numerical, of thin-walled steel members is mainly focused on stability analysis, i.e. buckling failure studies [164]. Yu and Schafer (2006) [165] classify instabilities of cold-formed sections in local, distortional and lateral-torsional buckling. However, for the design of cold-formed sections sometimes only local plate buckling modes is considered as the limiting phenomenon [50]; within this context, the two most common design methods are the Effective Width Method (EWM) [166] and the Direct Strength Method (DSM) [167]. Moen and Schafer (2009) extended the Direct Strength Method for members with perforations [168,169]. However, the prediction of residual stresses is hard to tackle due to some reasons: (i) information from manufacturers is not easy to obtain; (ii) real machines consist of many complex rolling stations; and the influence of other secondary processes can be significant, e.g. coiling [56], flattening [34] or pre-punching [170]. Roll forming is an especially complex process for modelling purposes in comparison to press braking; the progressive bending throughout the stations implies a three-dimensional deformation pattern so longitudinal effects can be critical. Thus, the validity of pure bending assumptions must be carefully assessed.

In the following subsections, modelling of roll forming dealing with residual stress predictions is reviewed, both considering analytical or semi-analytical expressions (Section 3.2) and Finite Element framework (Section 3.3). However, the fundamentals of strip deformation during roll forming are previously revisited (Section 3.1) with the aim of introducing the relationship between roll optimisation and strain minimisation. Finally, in Section 3.4, residual stress input in structural modelling is briefly discussed.

3.1. Theory of strip deformation in roll-forming

This section refers to the numerical-analytical procedures that can be exploited to analyse strip deformation during the roll-forming process as a previous step before the more accurate but more challenging Finite Element modelling. Due to the high computational cost of FE

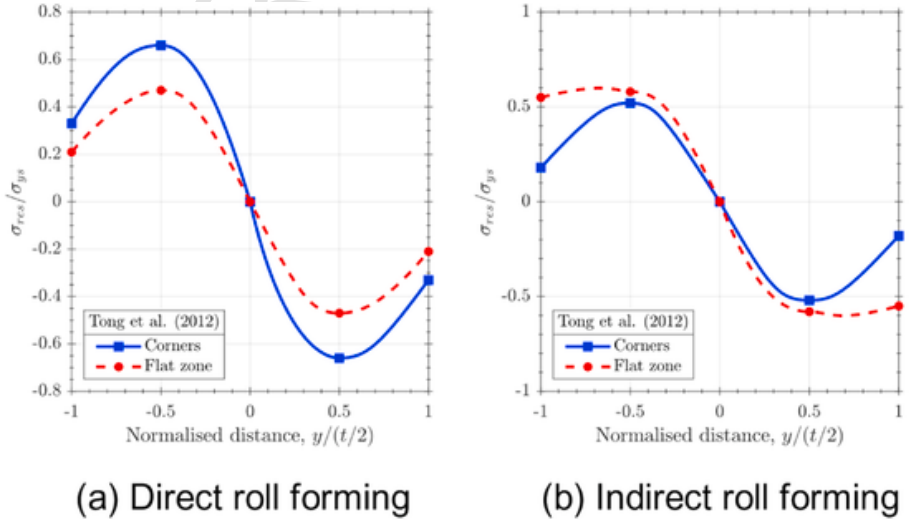

Fig. 12. Longitudinal residual stress through the thickness of a SHS, extracted from Tong et al. (2012) [142]. Simplified through-thickness symmetric distributions are considered after averaging hole drilling and X-ray diffraction measured points over the section.

simulations, the design of rolls still relies on theory of deformations, along flower-pattern assumptions and a simplified flow of material between stations. A detailed review of strip deformation theory in roll-forming can be found in the handbook of Halmos (2005) [17] and in the literature survey of Lindgren's thesis (2009) [171].

The deformation of the strip can be theoretically assumed uniform between stations. In that case, the elongation of the flange end can be determined following geometrical arguments [17]. However, the real flow behaviour of the metal strip deviates from the theoretical value predicted by geometry. The deformation between rolling stations is not progressive and is limited to a length L_e before entering the following forming roll. Bhattacharyya et al. (1983) [172] derived a simple analytical expression for a U-channel by minimising the work consumed during deformation phenomena:

$$L_e = l_f \sqrt{\frac{8\Delta\theta}{3t}} \# \tag{6}$$

where l_f is the flange length, t is the section thickness and $\Delta\theta$ is the bending angle increment. This parameter dependency was experimentally validated for mild steel and aluminium sections [172].

The number of passes determines the angle increment and is related to deformation behaviour and thus to the presence of residual stresses. "Forming angle method", which is based on geometrical relationships and the limitation of the forming angle, is sometimes used to assign a number of rolling stations [171]. Other methods consider empirical relationships for the selection of the number of forming steps [17,171]. Longitudinal strains have been measured by some authors during rolling [173]. Even though the present review is focused on residual stresses, the longitudinal residual stress will be clearly determined by this deformation behaviour.

A first approach to model the deformed strip is to define a normalised shape function; this strategy was firstly proposed by Kiuchi (1973) [174,175] and it has been adopted later by many authors [171,176] naming the method as "deformed curved surface" or DCS [17]. Duggal (1996) [177] implemented this expression to find the strain distribution during rolling using the finite difference method. A surface $S(x)$ is defined for each position between rolling stations:

$$S(x) = \sin\left[\frac{\pi}{2}\left(\frac{x}{L}\right)^n\right] \# \tag{7}$$

where L is the forming length, i.e. the distance between consecutive stations, x the axial coordinate and n is a forming coefficient. As an illustrative example, DCSs modelling the forming of a U-shape from a flat sheet is shown in Fig. 13 for different n coefficients. In this figure, the flower approach is not considered and the initial and only an initial and final rolling stations are considered for the U-section forming.

In order to select the forming coefficient n that simulates the real material flow, the power of deformation $\dot{W}$ must be minimised; values of n between 2 and 10 are obtained [17] depending the section shape and thickness. The DCS predictions for real n values confirm the fact that the deformation is not progressive and is limited to a length near the forming roll, as predicted by the expression derived by Bhattacharyya et al. (1983) [172]. A similar approach is considered by Nefussi and Gilormini (1993) [178] but using a kinematic approach and theory of shells to simulate the deformed strip shape during roll forming. DCS modelling procedures facilitate the determination of strain history during rolling and, when yielding behaviour is implemented, the residual strains and stresses. However, the usual procedure is limited to distribute longitudinal strains equally throughout rolling stations and to keep these strain peaks within the elastic range [171]. An extension of these methods was proposed by Liu et al. (2001) [179] including elastic-plastic B-spline large deformation theory.

COPRA software is one of the most used tools for the simulation of roll forming. It includes a Deformation Technology Module (DTM) in which the longitudinal strain peaks are determined taking into account not only the section shape but also roll diameter, material and thickness [180]. The determination of strain course is used to optimise the flower pattern for different section thicknesses and materials [181,182]. An example of the evolution of longitudinal flange strain during roll forming is shown in Fig. 14. This computer simulation is based on the Hauschild method, presented as an evolution of Kiuchi's approach in which inhomogeneous strain is included [180]. However, the physical-mathematical model is not provided by the developer.

It can be concluded that the aim of strip deformation modelling is not the determination of residual stresses. This preliminary design step is directed to minimise the longitudinal strain peak and theory on strip deformation is rarely connected to the prediction of residual stresses.

3.2. Analytical modelling of residual stresses

Moen et al. (2008) [34] presented a mathematical-mechanical framework for analytically predict through-thickness residual stresses in cold-formed open sections. The corners in the section bend plastically during the cold-forming process and, for a low R/t ratio, can be guaranteed that the sheet fully yields through its thickness in the corners. The following expressions are extracted and summarized from the mathematical derivation by Moen et al. (2008) [34]. The stresses in the bending direction, i.e. the transversal stresses, are obtained considering a perfectly plastic distribution:

$$\sigma_{trans}^{bend} = -\sigma_y y / |y| \# \tag{8}$$

where y is the through-thickness position and σ_y is the yield stress. The negative sign in (8) arises because the outer surface, which is under

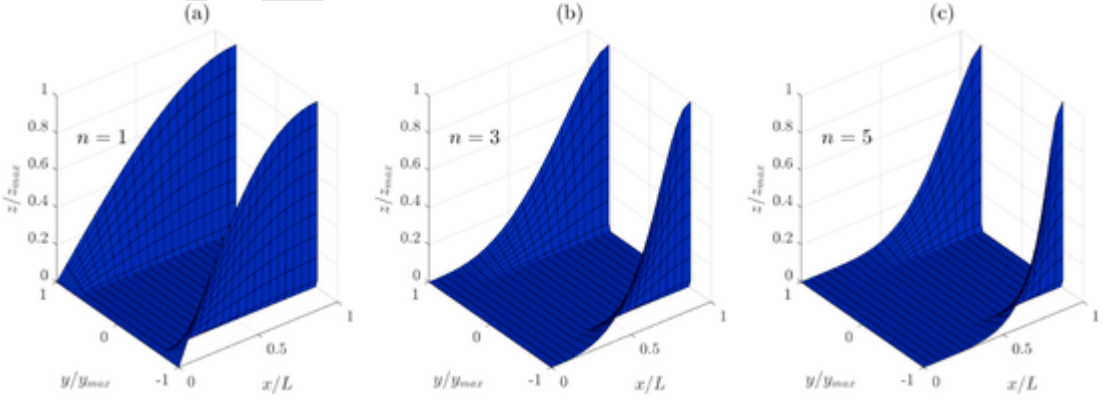

Fig. 13. Deformed strip from a flat sheet to a U-section considering $S(x)$ as in equation (7) for different n exponents: (a) $n = 1$, (b) $n = 3$ and (c) $n = 5$.

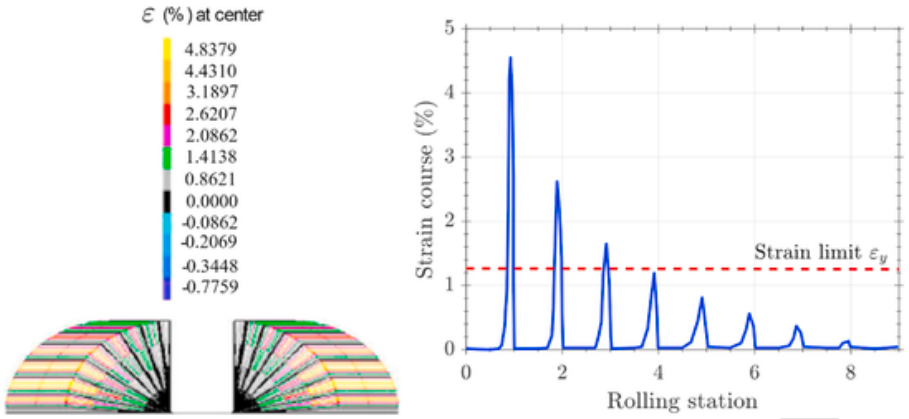

Fig. 14. Longitudinal flange deformation during forming passes simulated in COPRA and the corresponding section flower [182].

tension during bending, is assumed here in $y = -t/2$. That plastic distribution gives a moment M_{bend} that determines the elastic springback:

$$\sigma_{trans}^{springback} = \frac{M_{bend}}{I} y = \frac{\sigma_y t^2/4}{t^3/12} y = \frac{3\sigma_y y}{t} \# \tag{9}$$

where t is the section thickness and I the inertia of the sheet cross section. Moen et al. (2008) [34] also derived stresses for coiling, uncoiling and flattening processes. The stresses due to the coiling depend on the radial location of the analysed strip within the coil. The elastic core, c, might be defined as the inner part of the section where plastic strain has not been reached:

$$c = 2R_{coil}\sigma_y/E \leq t \# \tag{10}$$

where E is the Young's modulus. If the coil radius R_{coil} is small, almost the whole section is plasticized during coiling. The elastic-perfectly plastic distribution of stresses through the thickness due to longitudinal coiling is thus:

$$\sigma_{long}^{coil} = \begin{cases} \sigma_y y/(c/2), |y| < c/2 \\ \sigma_y y/|y|, |y| \geq c/2 \end{cases} \# \tag{11}$$

The uncoiling stresses might be found considering the elastic springback determined by the plastic coiling moment:

$$\sigma_{long}^{uncoil} = -\frac{12M_{coil}y}{t^3} = \frac{12\sigma_y y}{t^3}\left[\left(\frac{t}{2}\right)^2 - \frac{1}{3}\left(\frac{c}{2}\right)^2\right] \# \tag{12}$$

After uncoiling, the sheet still has a remaining curvature, R_{uncoil}, if the initial coil radius was too small. When the sheet enters the first roll, the stress applied for flattening is:

$$\sigma_{long}^{flatten} = -E\frac{y}{R_{uncoil}} = -Ey\left[\left(\frac{1}{R_{coil}}\right) - \left(\frac{M_{coil}}{EI}\right)\right] \# \tag{13}$$

The final distribution before rolling process, i.e. the sum of the three stress distributions ($\sigma_{long}^{c+u+f} = \sigma_{long}^{coil} + \sigma_{long}^{uncoil} + \sigma_{long}^{flatten}$), will depend mainly on the yield stress, the thickness and the coil radius. The last parameter is different for each sample location in the coil so this must be taken into account in the analysis of experimental results. The total analytical stresses are therefore the sum of all the stages during manufacturing. For the longitudinal and the transversal components:

$$\sigma_{long}^{res} = \sigma_{long}^{c+u+f} + 0.5\sigma_{trans}^{bend} + \nu\sigma_{trans}^{springback} \# \tag{14}$$

$$\sigma_{trans}^{res} = \nu\sigma_{long}^{c+u+f} + \sigma_{trans}^{bend} + \sigma_{trans}^{springback} \# \tag{15}$$

For the corresponding longitudinal stresses, a different coefficient ν is considered for the plastic bending than for the elastic springback. The representation of results for different coil radii is shown in Fig. 15a and b for the longitudinal and the transversal residual stresses, respectively. The influence of coiling is significative near the surfaces for a small coiling radius. As shown in that figure, the influential parameter is R_{coil}/t rather than the absolute radius.

The simplifications assumed for the predicted residual stresses plotted in Fig. 15 must be taken into account. An elastic perfectly plastic

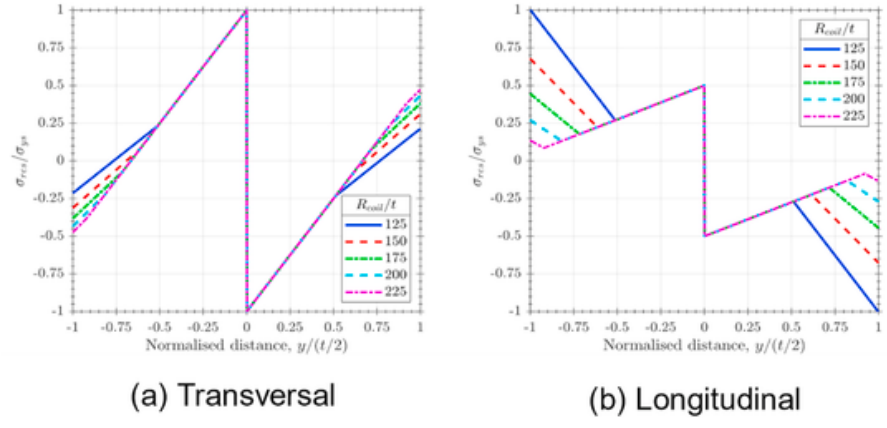

Fig. 15. Analytical trough-thickness distribution for: (b) transversal residual stresses and (b) longitudinal residual stresses, following Moen et al. (2008) [34] and considering different coiling radii.

behaviour has been modelled so hardening phenomena are neglected. To include more complex constitutive models, numerical and iterative procedures are required [183]. Moreover, even though that work aims at studying roll-forming [34], only a 2D pure bending is considered, with the associated Poisson effect and the subsequent elastic springback; the progressive longitudinal deformation actually taking place during roll-forming is not reproduced by the equations presented above. Thus, Fig. 15 can be validated with the experimental measurement of press-braked sections but the comparison with roll-formed sections can be problematic. Additionally, these expressions neglect thickness reduction and the shift of the neutral axis that plastic bending promotes. Nevertheless, an important conclusion of the simple analytical approach is that the linear simplification assumed by some authors [34] barely reproduces the zig-zag distribution produced by bending and springback. However, many experimental works measuring residual stresses only on the section surface, both using destructive or non-destructive techniques, still divide residual stresses in bending and membrane components.

In order to improve the accuracy of through-thickness distributions, Ingvarson (1975) [83] proposed a theoretical elastic-plastic framework and an incremental computer analysis to solve the Prandtl-Reuss flow rule with von Mises yield criterion and to determine residual stresses due to cold bending. Rondal (1987) [184] and Amouzegar et al. (2016) [35] presented a similar incremental numerical algorithm. Residual stresses are obtained in polar coordinates without the need of neglecting hardening, as in Moen et al. (2008) [34]. The determination of through-thickness distributions requires an incremental algorithm, so it cannot be regarded as an analytical procedure, but the flowchart requires less computational cost than finite element simulations.

As shown in Fig. 16, results from Amouzegar et al. (2016) [35] predict a non-linear zig-zag distribution that match reasonably the finite element (FE) distribution from Quach et al. (2006) [185] and the experimental findings of Weng and White (1990) using hole drilling and sectioning methods [64], which have been previously presented in Fig. 9. This model predicts, in contrast to the analytical expressions extracted from Moen et al. (2008) [34], a shift of the neutral axis towards the inner surface, i.e. $\sigma = 0$ for $y \approx 0.25 \times t/2$. This fact has been theoretically studied in bent corners [186,187] which is usually modelled considering a k-factor [188] and is experimentally accompanied by a reduction in sheet thickness [189,190]. Bend allowance is the term referring to the strip elongation during plastic bending [191] that limits the minimum bending radius [187] and also produces a thickness reduction at corners. It is common in manufacturing research on metal sheet bending to explore bendability and springback behaviour rather than the presence of residual stresses, even though these phenomena are interconnected. Residual stresses are strongly influenced by the unloading process and springback is a complex phenomenon that has been tried to be modelled considering different elastic-plastic frameworks [186], e.g. cyclic plasticity [192] or variable Young's modulus [193], and loading conditions [194]. Research on constitutive models, material properties and numerical procedures dealing with springback predictions has been reviewed by Wagoner et al. [195–197]. Zhang et al. (1998) [183] considered the influence of deformation history, i.e. repeated bending and reverse bending, on the springback behaviour and thus on the development of residual stress distributions. All these works consider plane strain conditions (see Fig. 17).

It must be noted that numerical and experimental results presented in Fig. 16 have been obtained for press braking, i.e. for pure 2D bending without longitudinal rolling effects; hence, this methodology proposed by Amouzegar et al. (2016) [35] is a great alternative to FE simulations of press braking but it would be limited for prediction in roll-formed sections.

Quach et al. (2004) [55] also derived a closed-form analytical solution for residual stresses due to coiling and uncoiling operation, validated by finite element simulations. Strain hardening is neglected in Ref. [55] but von Mises yield criterion and Prandtl-Reuss flow rule are considered. Additionally, equivalent plastic strain is integrated for each through-thickness point [55]. Quach et al. (2009a, 2009b) [56,198] combined the coiling – uncoiling solution with an analytical methodology to predict residual stresses due to press braking so the complete manufacturing process is reproduced for press-braked sections. Expressions modelling transverse bending during press braking considered both large and small-strain formulations and the Hill's anisotropic yield criterion.

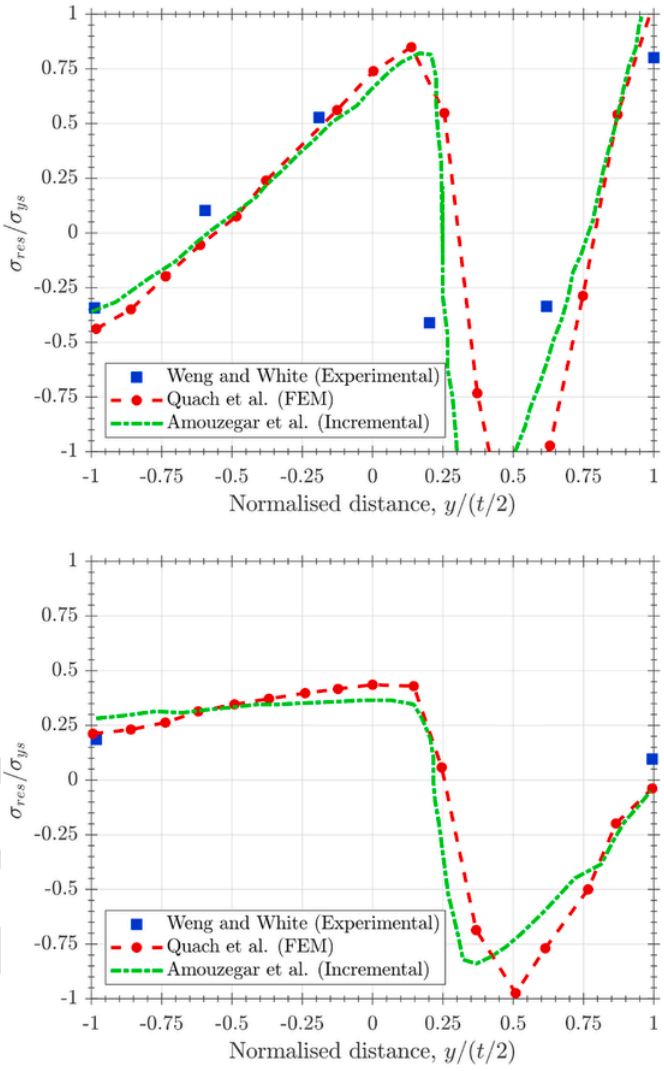

Fig. 16. Comparison of through-thickness residual stresses predicted by Weng and White (1990) using hole drilling and sectioning methods [64], by Quach et al. (2006) [185] using finite element simulations and by Amouzegar et al. (2016) [35] using an incremental method.

Analytical distributions proposed for stainless steel channel sections in Quach et al. (2009b) [198] that are based on large-strain formulation agree with FE results even for high curvatures, i.e. $R/t < 10$, where R is the bending or corner radius and t is the section thickness, so they can be regarded as accurate predictions for sharp corners. However, analytical stresses from a small-strain formulation provide significative errors in comparison to FE distributions for sharp corners and can only be used to predict residual stresses for low curvature, i.e. $R/t \geq 10$.

Additionally, all the analytical methodologies presented above are focused on the rolling forming and press braking of sections from mother coils to produce channel members, i.e. open sections. However,

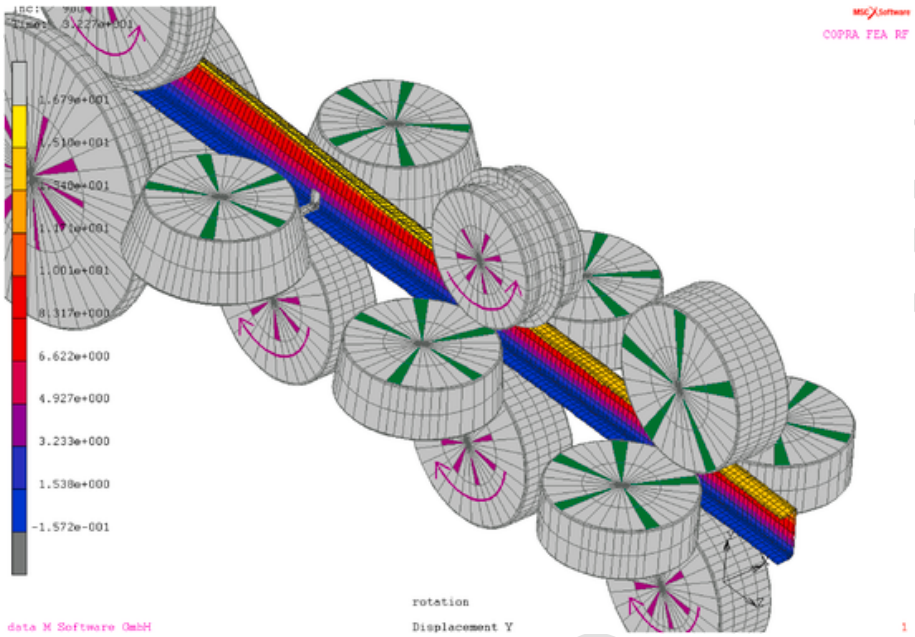

Fig. 17. Roll forming simulation in COPRA RF FEA considering friction and including driven rolls (purple with arrows) and idle rolls (green without arrows) [228]. (For interpretation of the references to colour in this figure legend, the reader is referred to the Web version of this article.)

many of the experimental methods discussed in Section 2 are focused on hollow sections. Typically, circular sections are produced from rolling and are then closed by seam welding [199]. Finally, the closed circular hollow section (CHS) is cold-rolled again [142] until the final elliptical [67,95], rectangular [63,66] or square [37,145] shape is obtained. This procedure is sometimes termed as continuous [200] or indirect forming, as already mentioned for the results presented by Tong et al. (2012) [142]. For rectangular (RHS) and square hollow sections (SHS), a direct-forming alternative is possible in which the desired shape is directly obtained in a single roll forming sequence and weld joining of the section lips is performed at the end. In this direct operation cold working is concentrated in the corners [200] whereas continuous or indirect strategy involves uniform bending during the first step to shape a circular section.

In order to predict the influence of the real strain history during manufacturing operations, the complete forming sequence must be considered. The first bending stages, from the input sheet to the circular hollow section, can be modelled considering the same principles already exposed for a concentrated bent corner but this time for small-curvature pure bending, i.e. for high bending radius. Thus, analytical closed-form solutions are similar to those used for coiling-uncoiling operations proposed by Quach et al. (2004) [55]. Quach et al. (2010) [201] proposed to extend this strategy for the prediction of residual stresses due to transverse bending in cold-formed CHSs, considering small-strain formulations, assuming plane strain, and including strain hardening and anisotropic plasticity. The detailed formulation adapted to transverse bending of CHS can be found in the work of Cai (2009) [202].

Welding influence on residual stresses is out of the scope of the present review, but seam joints will surely produce thermal stresses. Additionally, it must be noted that residual stresses are expected to increase in the welding line of a hollow section due to the constraint and corresponding reaction force [145] in comparison to a similarly welded plate. Moreover, modelling the final roll forming process of the closed circular section to obtain the desired shape, i.e. the last stage of indirect forming, is complex due to the absence of free edges and the corresponding constrained behaviour. Thus, to the knowledge of the authors, analytical approaches reproducing the real forming process from the already welded CHS to the final EHS, SHS or RHS shapes are unlikely so they are just based on local corner assumptions [203], i.e. high-curvature bending, that have been previously exposed. In order to evaluate how constraint effects might produce different residual stresses between open or closed sections under the same local small-curvature bending, Finite Element models are required.

3.3. Finite element modelling

Residual stress modelling of cold forming process is challenging because several reasons: (i) contact modelling between tools and the metal sheet influences solution; (ii) tools, die and punch in press braking and rolls in roll forming, are usually modelled as rigid analytical surfaces so the implications of the non-deformability assumption must be discussed; (iii) elastic-plastic constitutive models are crucial for the prediction of residual stresses; isotropic hardening is usually assumed even though unloading phenomena will deviate from that behaviour if kinematic effects, e.g. Bauschinger effects, are happening in reality; (iv) mesh refinement near corners and through-thickness. A very fine mesh critically increases the computation time; (v) implicit schemes exhibit convergence issues and longer computational time whereas explicit solver can cause error accumulation.

3.3.1. Press braking simulations

The need of a robust finite element framework for press braking is lower than for roll forming because the former process is accurately approximated by analytical or incremental algorithms considering pure bending, as shown in the previous section and in Fig. 16. However, some geometrical and material effects can be important and require finite element simulations.

Quach et al. [185] determined through FE simulations the presence of residual stresses for press-braked steel members. 2D simulations were carried out in ABAQUS using plane strain elements and symmetry boundary conditions. These authors successfully reproduced two benchmarking works, from Weng and Pekoz (1990) [82] and from Weng and White (1990) [64] and they perform a very rigorous mesh convergence study, adopting 16 elements in the corner region for the thickness direction. Both punch and lower die were modelled as analyt-

ical rigid surfaces and considering a hard contact with the sheet. For the simulation of consecutive bending steps in the lipped channel, the section must be rotated and the corresponding boundary conditions applied. Additionally, in the work of Quach et al. [185] coiling-induced residual stresses that have been predicted by analytical expressions are introduced as an initial stress state in the FE model. Despite the pure bending occurring during press braking, Mutafi et al. (2018) [204] simulated a 3D model to analyse longitudinal residual strains and edge effects.

Simulations of press braking usually aiming at optimising the punch – die design. Bakhshi-Jooybari et al. (2009) compared the springback behaviour under a V or a U-die using ABAQUS and considering the Hill's anisotropic model. Similarly, Thipprakmas (2010) [205] studied the effects of punch height on the bending allowance so stress distribution is only a consequence of material flow but not the required magnitude. A commercial FE code DEFORM-2D with plane strain elements and an automatic remeshing was used, as in Ref. [206] for the study of spring-back/spring-go phenomena.

For air-bending forming, where the punch bends the metal sheet without reaching the lower die [207], the punch displacement is a critical process parameter. Miranda et al. (2018) [208] combined finite element simulations and artificial neural networks to predict optimum parameters and geometries; similarly, Fu et al. (2010) [209] used neural networks to analyse punch radius effects. It can be mentioned that air-bending is analogous to a 3-point bending test, so beam theory can be applied [210].

3.3.2. Roll forming simulations

Roll forming simulations are extremely CPU-time consuming in comparison to press braking due to the high number of contacts and the non-linearity of the process. The common commercial codes used for stress-strain analysis, e.g. ABAQUS or ANSYS, are not optimised for roll design and selection of the number of stations. Thus, specific codes have been developed for roll forming simulation. Brunet et al. (1998) [211] developed the code PROFIL for a finite element for a 3D shell analysis and obtained the strain history during rolling. However, this shell analysis cannot be used to study through-thickness residual stresses. UBECO-PROFIL has also been used as a pre-processor for the determination of bending sequence of a roll-formed U-channel, that is simulated in an implicit analysis in ABAQUS [212]. UBECO-PROFIL implements in new versions an interface to the explicit solver LS-DYNA to simulate roll forming. Sheu (2004) [213] used LS-DYNA to study the effect of rolling parameters, e.g. friction or speed, and Paralikas et al. (2011) [214] to analyse different flower patterns in a roll-formed advanced high strength steel. LS-DYNA is usually accessed through the ANSYS environment [214]. Spoorenberg et al. (2011) [215] have used an implicit scheme in ANSYS to simulate roll bending to estimate residual stresses in curved sections. However, roll bending is less demanding than roll forming in terms of contacts and non-linearities.

Ponthot (1995) [216] built the code METAFOR that implements an Arbitrary Lagrangian-Eulerian algorithm, reducing the required number of elements and the computational time in comparison to the classical Updated Lagrange approach [217,218]. This FE has been validated for roll forming simulations [219] and used by many authors. Bui and Ponthot (2008) [173] simulated the bend of a U-channel considering only one through-thickness layer since they only studied longitudinal strain, springback and final geometry. Rossi et al. (2013) [219] also performed simulations of a U-channel but considering 4 layers of elements for through-thickness meshing even though the objective was to analyse corner stress enhancement. However, some works using METAFOR for roll forming simulation still rely on the specific software COPRA to design flower patterns [220]. Sheikh and Palavilayil (2006) [221] used the FE software SHAPE-RF that includes an initial guessing algorithm for the 2D section before the 3D rigid-plastic finite element calculation. Heislitz et al. (1996) [222] employed the FE software PAM-STAMP which implements an explicit scheme and took advantage of mass scaling and adaptative mesh refinement for reducing computational time. This code has been compared with an implicit solver for simple bending problems providing similar results [223].

One of the most used software is COPRA-RF (see Fig. 17), developed by DataM, which follows a two-step flowchart: a pre-processing stage where the flower pattern is optimised and rolls are designed, and a calculation step that is integrated in the MSC Marc FE solver. A snapshot of this environment can be seen in Fig. 15. Therefore, finite element formulations, contact modelling, remeshing techniques or boundary conditions can be redefined exploiting MSC Marc capabilities. A bending sequence is generated, and the corresponding flower pattern, in COPRA-RF for the considered final cross-section. Some complex geometries are hard to tackle in the COPRA pre-processing; for example, Görtan et al. (2009) [224] defined the bending sequence of a branched section and directly used MSC Marc to simulate roll forming. Wiebenga et al. (2013) [225] also used this software for a V-section. Pastor et al. (2013) [226] simulated an upright section typical of racking structures. They used a single through-thickness element. Jiao-Jiao et al. (2020) [227] studied the springback of a roll-formed high-strength steel section using COPRA. Roll-forming simulation with COPRA can also be used to assess possible geometrical deviations between the real scanned section between passes and the simulated strip deformation [190]. Liu et al. (2018) [190] simulated roll-forming in COPRA to determine local thickness reduction and results were experimentally compared with hat-shaped sections formed through cold rolling. Bonada et al. (2015) [170] studied in COPRA the influence of perforations on roll forming and residual stress distributions. Simulations of flexible roll forming, i.e. when cross section of the final member is not constant, can also be performed by COPRA [7].

Wang et al. (2020) [146] used COPRA for the optimisation of the flower pattern and for the roll design but simulate rolling process including friction in ABAQUS Explicit. As already mentioned, these authors validated the numerical results through XRD measurements along the perimeter. The same strategy, i.e. bending sequence and roll design in COPRA and simulation in ABAQUS Explicit, is followed by Yan et al. (2017) [229].

Salmani Tehrani et al. (2006) [230] pointed out an advantage of ABAQUS Explicit, in which shell element thickness can be used for modelling contact problems. The authors analysed the longitudinal strain behaviour during roll forming considering localised buckling as a limiting phenomenon; they also verified that solution was not deviating from quasi-static conditions by computing the kinetic energy. Kang et al. (2014) [231] and Safdarian and Naeini (2015) [232] also employed shell elements and the ABAQUS Explicit solver. The anisotropic Hill's yield criterion was considered in Ref. [231].

Muller et al. (2011) [233] proposed a simplified 2D approach in ABAQUS in which each pass is independently simulated. Even though the material flow between stations is not simulated, springback after each pass was experimentally compared. An implicit scheme could be followed due to the reduced number of plane strain elements. It is important to highlight that roll forming is an expensive computational problem, so the understanding of lagrangian/eulerian formulations and meshing strategies is crucial. In addition, the limitations of explicit schemes [234], adopted in some works simulating roll forming [222], must be better discussed.

Regarding hollow sections, as discussed in Section 3.2, the manufacturing process can be direct or continuous (indirect). In the former case, the framework revisited above is valid but the simulation of the final operation of joining the section lips is required. On the other hand, FE simulations of continuous forming can be divided in the three corresponding stages: circular forming, welding and final shaping. As pointed out by Yao et al. (2019a) [235], numerical works on hollow

sections are scarce in comparison with simulations for steel open sections. The previously mentioned analytical solutions for coiling-uncoiling and transverse bending were considered by Yao et al. (2019a) [235] as the initial stress-strain state for welding and shaping simulations in ABAQUS. These simulations were performed using shell elements and 17 integration points, demonstrating that non-linear distributions of through-thickness residual stress can also be determined. Using this approach, simplified block distributions were proposed by Yao et al. (2020) [236] for elliptical hollow sections (EHS). Similarly, strength enhancement and local geometric imperfections can also be predicted considering this FE modelling framework for continuous forming [237]. Yao et al. (2019a) [235] also included a sequentially coupled thermal-stress analysis to reproduce electric resistance welding (ERW); these authors did not consider heat source models and a simplified temperature history approach was implemented. However, temperature-dependent properties, thermal expansion and annealing effects were taken into account. Through this methodology, negligible influence of ERW on residual stresses was numerically obtained [235].

Other forming parameters are also influential for rolling simulations. For instance, friction is reproduced by Hong et al. (2001) [238] using the Coulomb's friction model in COPRA with $\mu = 0.2$, as in Ref. [173,230]; Safdarian and Naeini (2015) [232] assessed different values (0.1, 0.15 and 0.2). Lubrication or forming velocity could influence friction properties [239]. The speed of the metal sheet can be imposed as a boundary condition [222] or can be governed by the rotation of rolls and friction phenomena [230]. In Ref. [225] the sheet enter with a speed of 0.0225 m/s for roll forming of a V section while top and bottom rolls are driven. In contrast, Safdarian and Naeini (2015) [232] studied higher speeds (1, 2 and 2.5 m/s), concluding that forming speed has not influence on material flow as long as quasi-static conditions [173] are verified and dynamic effects can be neglected. Therefore, rolls can be driven, i.e. rolls are moving the sheet, or rolls are non-driven, i.e. the sheet is "pushed" forward in the rolling direction [17]. Each roll on each station can be easily defined as driven or non-driven within COPRA simulations [240], so real machines can be better imitated.

Heating effects are neglected for roll forming because localised temperature raise due to the friction between rolls and the metal sheet is small enough to avoid an important thermal gradient and the corresponding residual stresses. Only for cold rolling with thickness reduction these effects must be considered [241].

Some authors have also modelled dimpling processes in cold-rolled forming [242]. Dimpled surfaces are produced before roll forming with the aim of improving mechanical performance of some structural members [243].

A mixed numerical-experimental methodology was proposed by Abvabi et al. [155,244,245] to quantify residual stresses before roll forming, i.e. stresses remaining after the preparatory operations. Considering the steel member response in pure bend tests, a residual stress distribution through the thickness is determined using an inverse numerical methodology.

3.3.3. Residual stress input in structural modelling

Finite element modelling of structural behaviour of cold-formed profiles is out of the scope of this work; an overview of elastic buckling and nonlinear collapse is given by Schafer et al. (2010) [69]. The authors highlight the importance of two physical features of cold forming – geometric imperfections and residual stresses – for collapse modelling. Some strategies for the implementation of residual stress distributions for the initial state of cold-formed member in structural modelling are here reviewed.

The inclusion of residual stresses as an initial field in Finite Element simulations may be difficult due to the lack of a complete 3D map and the complicated extrapolation. Narayanan and Mahendran (2003) [246] applied a residual stress field in a FE static analysis of cold-formed steel columns; they considered, following [51], residual stresses of 17% of the yield stress uniformly distributed along the section perimeters with tension on the outer surfaces and compression on the inner ones. They used the ABAQUS capability of establishing initial conditions by means of a user-defined subroutine for the initial stress field (SIGINI). Quach et al. (2010) [247] simulated nonlinear buckling of press-braked channels by implementing analytical solutions for residual stresses as initial conditions in ABAQUS. In flat regions only analytical expressions from coiling operations were considered [55], whereas corners were modelled assuming the local high curvature [198]. Yao et al. (2019b) [237] used the combination of analytical and Finite Element simulations, which has been discussed in Section 3.3.2 for reference [235], to study not only residual stresses, but also geometrical imperfections and strength enhancement [237]. The final state after FE simulation of the shaping process of elliptical hollow sections (EHS) was then translated as the initial state for the FE analysis of stub-column behaviour in ABAQUS [237].

Pastor et al. (2013) [170,226] transferred residual stresses that were determined in COPRA to an ANSYS model with the aim of studying buckling failure. A routine in Matlab was programmed to localise nodes and assign elastic-plastic strain tensors to the corresponding integration points in ANSYS. The same strategy is followed later by Bonada et al. (2015) [170].

On the other hand, some authors proposed blocks of longitudinal residual stresses, e.g. Thong et al. (2012) [142] or Cruise and Gardner (2008) [26] who collected bending longitudinal stresses in blocks and presented by Jandera et al. (2008) [144].

4. Conclusions

Literature survey and the discussion on experimental and numerical determination of residual stresses in cold-formed members lead to the following conclusions that summarise the state-of-the-art:

- Longitudinal stress distributions are required to better characterise the structural response of cold-formed members when buckling failures are assessed. Thus, research has being focused in the determination of longitudinal residual stresses, commonly using Sectioning methods. The strip cutting operations are not standardised and different approaches are found. Transversal sectioning is less common than longitudinal striping.
- Deep hole drilling (DHD) and ring core (RC) are infrequent for thin members due to larger or deeper range. Therefore, hole drilling is here revisited as the most advantageous semi-destructive technique for thin cold-formed profiles. This method is standardised, but some limitations are associated to the calibration coefficients determination.
- X-ray diffraction method is the most common way of determining surface residual stresses without the damage of the workpiece. However, layer removal and the corresponding correction is required to find through-thickness residual stresses.
- Modelling approaches for press braking and roll forming are very different because the latter is a 3D process in which strip deformation between rolls is a challenging topic for researchers whereas press braking can be assumed as a 2D pure bending. Theory on strip deformation has been introduced in Section 3.1 even though it is usually applied to roll design and optimisation, rather than to obtain residual stresses.
- Analytic expressions or incremental algorithms to find residual stresses are based on elastic-plastic constitutive models but usually rely on some simplifications. The mathematical framework proposed by different authors is a good approximation to the transverse and longitudinal stress evolution during coiling, uncoiling, flattening, bending and springback. For hollow sections, the continuous forming

stages must be considered. Nevertheless, these approaches are limited to a 2D bending and cannot be accurately used to reproduce roll forming.

- Finite element modelling of roll forming is a critical issue due to the high computational cost caused by the required mesh, the number of contacts and the non-linearities. For roll forming simulation, multi-purpose commercial software as ABAQUS, MSC Marc or ANSYS have been used.

Declaration of competing interest

The authors declare that they have no known competing financial interests or personal relationships that could have appeared to influence the work reported in this paper.

Acknowledgements

The authors gratefully acknowledge financial support from the FASTCOLD project (FAtigue STrength of COLD-formed structural steel details; Ref. 745982–2017) funded by Research Fund for Coal and Steel (RFCS) of the European Commission. A. Díaz wishes to thank the Department of Mechanical Engineering of the Faculty of Engineering from the University of Porto (FEUP) for providing hospitality during his post-doctoral research stay.

References

[1] C.L. Nilsen, M.A.O. Mydin, M. Ramli, Performance of lightweight thin-walled steel sections: theoretical and mathematical considerations, Adv. Appl. Sci. Res. 3 (2012) 2847–2859.
[2] A. Ghersi, R. Landolfo, F. Mazzolani, Design of Metallic Cold-Formed Thin-Walled Members, CRC Press, 2001.
[3] EN 1993–1–1, Eurocode 3: Design of steel structures-Part 1-1: general rules and rules for buildings, CEN (2005).
[4] Y.J. Guo, A.Z. Zhu, Y.L. Pi, F. Tin-Loi, Experimental study on compressive strengths of thick-walled cold-formed sections, J. Constr. Steel Res. 63 (2007) 718–723, doi:10.1016/j.jcsr.2006.08.008.
[5] EN 1993-1-3, Eurocode 3: Design of steel structures-Part 1-3: general rules-Supplementary rules for cold-formed members and sheeting, CEN (2006).
[6] K. Sweeney, U. Grunewald, The application of roll forming for automotive structural parts, J. Mater. Process. Technol. 132 (2003) 9–15, doi:10.1016/S0924-0136(02)00193-0.
[7] B. Abeyrathna, B. Rolfe, L. Pan, R. Ge, M. Weiss, Flexible roll forming of an automotive component with variable depth, Adv. Mater. Process. Technol. 2 (2016) 527–538, doi:10.1080/2374068X.2016.1247234.
[8] C.W. Shao, P. Zhang, Y.K. Zhu, Z.J. Zhang, Y.Z. Tian, Z.F. Zhang, Simultaneous improvement of strength and plasticity: additional work-hardening from gradient microstructure, Acta Mater. 145 (2018) 413–428, doi:10.1016/j.actamat.2017.12.028.
[9] D.L. McDowell, Multiscale modeling of interfaces, dislocations, and dislocation field plasticity, CISM Int. Cent. Mech. Sci. Courses Lect., Springer International Publishing, 2019, pp. 195–297, doi:10.1007/978-3-319-94186-8_5.
[10] R. Ibáñez, E. Abisset-Chavanne, D. González, J.L. Duval, E. Cueto, F. Chinesta, Hybrid constitutive modeling: data-driven learning of corrections to plasticity models, Int. J. Material Form. 12 (2019) 717–725, doi:10.1007/s12289-018-1448-x.
[11] E. Oñate, D. Peric, E. de Souza Neto, M. Chiumenti, Advances in Computational Plasticity: A Book in Honour of D. Roger J. Owen, Springer, 2017.
[12] X. Cheng, J.W. Fisher, H.J. Prask, T. Gnäupel-Herold, B.T. Yen, S. Roy, Residual stress modification by post-weld treatment and its beneficial effect on fatigue strength of welded structures, in: Int J. Fatigue (Ed.), Elsevier, 2003, pp. 1259–1269, doi:10.1016/j.ijfatigue.2003.08.020.
[13] C.P. Lamarche, R. Tremblay, Seismically induced cyclic buckling of steel columns including residual-stress and strain-rate effects, J. Constr. Steel Res. 67 (2011) 1401–1410, doi:10.1016/j.jcsr.2010.10.008.
[14] M.N. James, Residual stress influences on structural reliability, Eng. Fail. Anal. 18 (2011) 1909–1920, doi:10.1016/j.engfailanal.2011.06.005.
[15] M. Thirumurugan, S. Kumaran, S. Suwas, T.S. Rao, Effect of rolling temperature and reduction in thickness on microstructure and mechanical properties of ZM21 magnesium alloy and its subsequent annealing treatment, Mater. Sci. Eng. 528 (2011) 8460–8468, doi:10.1016/j.msea.2011.07.047.
[16] M. Abambres, W.M. Quach, Residual stresses in steel members: a review of available analytical expressions, Int. J. Struct. Integr. 7 (2016) 70–94, doi:10.1108/IJSI-12-2014-0070.
[17] G.T. Halmos, Roll Forming Handbook, Crc Press, 2005.
[18] B.B. He, B. Hu, H.W. Yen, G.J. Cheng, Z.K. Wang, H.W. Luo, M.X. Huang, High dislocation density-induced large ductility in deformed and partitioned steels, Science 80 (357) (2017) 1029–1032, doi:10.1126/science.aan0177.
[19] W.M. Quach, P. Qiu, Strength and ductility of corner materials in cold-formed stainless steel sections, Thin-Walled Struct. 83 (2014) 28–42, doi:10.1016/j.tws.2014.01.020.
[20] H.N. Trinh, G. Proust, C.H. Pham, Effect of manufacturing process on material properties at the corners of G450 cold-formed steel channel sections, Lect. Notes Civ. Eng., Springer, 2018, pp. 434–441, doi:10.1007/978-981-10-6713-6_43.
[21] P. Kusakin, A. Belyakov, C. Haase, R. Kaibyshev, D.A. Molodov, Microstructure evolution and strengthening mechanisms of Fe-23Mn-0.3C-1.5Al TWIP steel during cold rolling, Mater. Sci. Eng. 617 (2014) 52–60, doi:10.1016/j.msea.2014.08.051.
[22] B.L. Li, A. Godfrey, Q.C. Meng, Q. Liu, N. Hansen, Microstructural evolution of IF-steel during cold rolling, Acta Mater. 52 (2004) 1069–1081, doi:10.1016/j.actamat.2003.10.040.
[23] Y.F. Shen, C.H. Qiu, L. Wang, X. Sun, X.M. Zhao, L. Zuo, Effects of cold rolling on microstructure and mechanical properties of Fe-30Mn-3Si-4Al-0.093C TWIP steel, Mater. Sci. Eng. 561 (2013) 329–337, doi:10.1016/j.msea.2012.10.020.
[24] D. Zamani, A. Golshan, G. Dini, Z.N. Ismarrubie, M.A. Azmah Hanim, Z. Sajuri, Optimization of cold rolling and subsequent annealing treatment on mechanical properties of TWIP steel, J. Mater. Eng. Perform. 26 (2017) 3666–3675, doi:10.1007/s11665-017-2801-9.
[25] N. Nakada, H. Ito, Y. Matsuoka, T. Tsuchiyama, S. Takaki, Deformation-induced martensitic transformation behavior in cold-rolled and cold-drawn type 316 stainless steels, Acta Mater. 58 (2010) 895–903, doi:10.1016/j.actamat.2009.10.004.
[26] R.B. Cruise, L. Gardner, Residual stress analysis of structural stainless steel sections, J. Constr. Steel Res. 64 (2008) 352–366, doi:10.1016/j.jcsr.2007.08.001.
[27] R. Nandan, R. Rai, R. Jayakanth, S. Moitra, N. Chakraborti, A. Mukhopadhyay, Regulating crown and flatness during hot rolling: a multiobjective optimization study using genetic algorithms, Mater. Manuf. Process. 20 (2005) 459–478, doi:10.1081/AMP-200053462.
[28] M.P. Guerrero, C.R. Flores, A. Pérez, R. Colás, Modelling heat transfer in hot rolling work rolls, J. Mater. Process. Technol. 94 (1999) 52–59, doi:10.1016/S0924-0136(99)00083-7.
[29] G.Y. Tzou, M.N. Huang, Study on minimum thickness for asymmetrical hot-and-cold PV rolling of sheet considering constant shear friction, J. Mater. Process. Technol. 119 (2001) 229–233, doi:10.1016/S0924-0136(01)00965-7.
[30] M.S. Mohsen, B.A. Akash, Energy analysis of the steel making industry, Int. J. Energy Res. 22 (1998) 1049–1054, doi:10.1002/(SICI)1099-114X(19981010)22:12<1049::AID-ER422>3.0.CO;2-W.
[31] J. Becque, Optimization of cold-formed steel products: achievements, challenges and opportunities, Ce/Papers 3 (2019) 211–218, doi:10.1002/cepa.1048.
[32] M. Ashraf, L. Gardner, D.A. Nethercot, Strength enhancement of the corner regions of stainless steel cross-sections, J. Constr. Steel Res. 61 (2005) 37–52, doi:10.1016/j.jcsr.2004.06.001.
[33] M.A. Dar, D.K. Ashish, A.R. Dar, A Study on cold formed steel Beams-A review, I-Manager's, J. Struct. Eng. 3 (2014) 34.
[34] C.D. Moen, T. Igusa, B.W. Schafer, Prediction of residual stresses and strains in cold-formed steel members, Thin-Walled Struct. 46 (2008) 1274–1289, doi:10.1016/J.TWS.2008.02.002.
[35] H. Amouzegar, B.W. Schafer, M. Tootkaboni, An incremental numerical method for calculation of residual stresses and strains in cold-formed steel members, Thin-Walled Struct. 106 (2016) 61–74, doi:10.1016/j.tws.2016.03.019.
[36] G.J. Hancock, T. Murray, D.S. Ellifrit, Cold-formed Steel Structures to the AISI Specification, CRC Press, 2001.
[37] P.W. Key, G.J. Hancock, A theoretical investigation of the column behaviour of cold-formed square hollow sections, Thin-Walled Struct. 16 (1993) 31–64, doi:10.1016/0263-8231(93)90040-H.
[38] F. Nishino, L. Tall, Residual stress and local buckling strength OF steel columns, Proc. Japan Soc. Civ. Eng. 1969 (1969) 79–96, doi:10.2208/jscej1969.1969.172_79.
[39] H. Jiao, X.L. Zhao, Imperfection, residual stress and yield slenderness limit of very high strength (VHS) circular steel tubes, J. Constr. Steel Res. 59 (2003) 233–249, doi:10.1016/S0143-974X(02)00025-1.
[40] S.K. Cho, Y.S. Yang, K.J. Son, J.Y. Kim, Fatigue strength in laser welding of the lap joint, Finite Elem. Anal. Des. 40 (2004) 1059–1070, doi:10.1016/j.finel.2003.08.010.
[41] S. Song, P. Dong, Residual stresses at weld repairs and effects of repair geometry, Sci. Technol. Weld. Join. 22 (2017) 265–277, doi:10.1080/13621718.2016.1224544.
[42] A. Valiente, Fracture and fatigue failure in the Spanish codes for design of steel structures, Eng. Fail. Anal. 16 (2009) 2658–2667, doi:10.1016/j.engfailanal.2009.04.025.
[43] S.J. Maddox, Influence of tensile residual stresses on the fatigue behavior of welded joints in steel, Residual Stress Eff. Fatigue, ASTM International, 1982.
[44] EN 1993–1–9, Eurocode 3: design of steel structures—part 1–9: fatigue, CEN (2005).
[45] R.A. LaBoube, W. Yu, Design of Cold-Formed Steel Structural Members and Connections for Cyclic Loading (Fatigue), 1999.
[46] K.H. Klippstein, Fatigue behavior of steel-sheet fabrication details, SAE Tech. Pap., SAE International, 1981, doi:10.4271/810436.
[47] K.H. Klippstein, Fatigue of fabricated steel-sheet details—phase II, SAE Trans. 94 (1985) 52–70, doi:10.2307/44721549.
[48] Y.H. Lee, C.S. Tan, S. Mohammad, M. Md Tahir, P.N. Shek, Review on cold-formed steel connections, Sci. World J. 2014 (2014) 951216, doi:10.1155/2014/951216.
[49] D. Dubina, V. Ungureanu, Effect of imperfections on numerical simulation of instability behaviour of cold-formed steel members, Thin-Walled Struct. 40 (2002) 239–262, doi:10.1016/S0263-8231(01)00046-5.

[50] E. de M. Batista, Local-global buckling interaction procedures for the design of cold-formed columns: effective width and direct method integrated approach, Thin-Walled Struct. 47 (2009) 1218–1231, doi:10.1016/j.tws.2009.04.004.

[51] B.W. Schafer, T. Peköz, Computational modeling of cold-formed steel: characterizing geometric imperfections and residual stresses, J. Constr. Steel Res. 47 (1998) 193–210, doi:10.1016/S0143-974X(98)00007-8.

[52] G. Zeng, S.H. Li, Z.Q. Yu, X.M. Lai, Optimization design of roll profiles for cold roll forming based on response surface method, Mater. Des. 30 (2009) 1930–1938, doi:10.1016/j.matdes.2008.09.018.

[53] J.H. Wiebenga, J.H. Wiebenga, Robust Design and Optimization of Forming Processes, 2014. www.m2i.nl. (Accessed 27 April 2020).

[54] J.H. Wiebenga, E.H. Atzema, Y.G. An, H. Vegter, A.H. Van Den Boogaard, Effect of material scatter on the plastic behavior and stretchability in sheet metal forming, J. Mater. Process. Technol. 214 (2014) 238–252, doi:10.1016/j.jmatprotec.2013.08.008.

[55] W.M. Quach, J.G. Teng, K.F. Chung, Residual stresses in steel sheets due to coiling and uncoiling: a closed-form analytical solution, Eng. Struct. 26 (2004) 1249–1259, doi:10.1016/j.engstruct.2004.04.005.

[56] W.M. Quach, J.G. Teng, K.F. Chung, Residual stresses in press-braked stainless steel sections, I: coiling and uncoiling of sheets, J. Constr. Steel Res. 65 (2009) 1803–1815, doi:10.1016/j.jcsr.2009.04.007.

[57] N.S. Rossini, M. Dassisti, K.Y. Benyounis, A.G. Olabi, Methods of measuring residual stresses in components, Mater. Des. 35 (2012) 572–588, doi:10.1016/J.MATDES.2011.08.022.

[58] G.S. Schajer, Practical Residual Stress Measurement Methods, wiley, Chichester, UK, 2013, doi:10.1002/9781118402832.

[59] G. Roy, D. Polyzois, M. Mohamedien, Residual stresses in cold formed steel sections, International Specialty Conference on Cold-Formed Steel Structures 5 (1994) 691–703.

[60] C. Bouffioux, R. Pesci, R. Boman, N. Caillet, J.P. Ponthot, A.M. Habraken, Comparison of residual stresses on long rolled profiles measured by X-ray diffraction, ring core and the sectioning methods and simulated by FE method, Thin-Walled Struct. 104 (2016) 126–134, doi:10.1016/j.tws.2016.03.017.

[61] R.B. Cruise, L. Gardner, Strength enhancements induced during cold forming of stainless steel sections, J. Constr. Steel Res. 64 (2008) 1310–1316, doi:10.1016/j.jcsr.2008.04.014.

[62] S. Afshan, B. Rossi, L. Gardner, Strength enhancements in cold-formed structural sections — Part I: material testing, J. Constr. Steel Res. 83 (2013) 177–188, doi:10.1016/j.jcsr.2012.12.008.

[63] X.Z. Zhang, S. Liu, M.S. Zhao, S.P. Chiew, Comparative experimental study of hot-formed, hot-finished and cold-formed rectangular hollow sections, Case Stud. Struct. Eng. 6 (2016) 115–129, doi:10.1016/j.csse.2016.09.001.

[64] C.C. Weng, R.N. White, Residual stresses in cold-bent thick steel plates, J. Struct. Eng. 116 (1990) 24–39, doi:10.1061/(ASCE)0733-9445(1990)116:1(24).

[65] N. Tebedge, G. Alpsten, L. Tall, Residual-stress measurement by the sectioning method, Exp. Mech. 13 (1973) 88–96, doi:10.1007/BF02322389.

[66] J.L. Ma, T.M. Chan, B. Young, Material properties and residual stresses of cold-formed high strength steel hollow sections, J. Constr. Steel Res. 109 (2015) 152–165, doi:10.1016/j.jcsr.2015.02.006.

[67] W.-M. Quach, B. Young, Material properties of cold-formed and hot-finished elliptical hollow sections, Adv. Struct. Eng. 18 (2015) 1101–1114, doi:10.1260/1369-4332.18.7.1101.

[68] R.C. Spoorenberg, H.H. Snijder, J.C.D. Hoenderkamp, Experimental investigation of residual stresses in roller bent wide flange steel sections, J. Constr. Steel Res. 66 (2010) 737–747, doi:10.1016/j.jcsr.2010.01.017.

[69] B.W. Schafer, Z. Li, C.D. Moen, Computational modeling of cold-formed steel, Thin-Walled Struct. 48 (2010) 752–762, doi:10.1016/j.tws.2010.04.008.

[70] S. Heinilä, T. Björk, G. Marquis, R. Neu, K. Wallin, S. Thompson, S.W. Dean, The influence of residual stresses on the fatigue strength of cold-formed structural tubes, J. ASTM Int. (JAI) 5 (2008) 101570, doi:10.1520/JAI101570.

[71] Y. Ueda, K. Fukuda, K. Nakacho, S. Endo, A new measuring method of residual stresses with the aid of finite element method and reliability of estimated values, J. Soc. Nav. Archit. Jpn. 1975 (1975) 499–507.

[72] Y. Ueda, K. Fukuda, M. Tanigawa, New measuring method of three dimensional residual stresses based on theory of inherent strain (welding mechanics, strength & design), Trans. JWRI 8 (1979) 249–256.

[73] Y. Ueda, M.G. Yuan, Prediction of Residual Stresses in Butt Welded Plates Using Inherent Strains, 1993.

[74] M.R. Hill, D. V Nelson, The inherent strain method for residual stress determination and its application to a long welded joint, ASME-PUBLICATIONS-PVP 318 (1995) 343–352.

[75] M.R. Hill, D. V Nelson, The localized eigenstrain method for determination of triaxial residual stress in welds, ASME-PUBLICATIONS-PVP 373 (1998) 397–404.

[76] G. Ivetic, A. Lanciotti, C. Polese, Electric strain gauge measurement of residual stress in welded panels, J. Strain Anal. Eng. Des. 44 (2009) 117–126, doi:10.1243/03093247JSA456.

[77] O. Muránsky, C.J. Hamelin, F. Hosseinzadeh, M.B. Prime, Mitigating cutting-induced plasticity in the contour method. Part 2: numerical analysis, Int. J. Solid Struct. 94–95 (2016) 254–262, doi:10.1016/j.ijsolstr.2015.12.033.

[78] F. Hosseinzadeh, Y. Traore, P.J. Bouchard, O. Muránsky, Mitigating cutting-induced plasticity in the contour method, part 1: Experimental, Int. J. Solid Struct. 94–95 (2016) 247–253, doi:10.1016/j.ijsolstr.2015.12.034.

[79] Y.L. Sun, M.J. Roy, A.N. Vasileiou, M.C. Smith, J.A. Francis, F. Hosseinzadeh, Evaluation of errors associated with cutting-induced plasticity in residual stress measurements using the contour method, Exp. Mech. 57 (2017) 719–734, doi:10.1007/s11340-017-0255-5.

[80] Y.B. Wang, G.Q. Li, S.W. Chen, The assessment of residual stresses in welded high strength steel box sections, J. Constr. Steel Res. 76 (2012) 93–99, doi:10.1016/j.jcsr.2012.03.025.

[81] D. Dat, T. Peköz, The strength of cold-formed steel columns, Center for ColdFormed Steel Structures Library 110 (1980).

[82] C.C. Weng, T. Pekoz, Residual stresses in cold-formed steel members, J. Struct. Eng. 116 (1990) 1611–1625.

[83] L. Ingvarsson, Cold-forming Residual Stresses Effect on Buckling, 1975.

[84] E. de M. Batista, F.G. Rodrigues, Residual stress measurements on cold-formed profiles, Exp. Tech. 16 (1992) 25–29, doi:10.1111/j.1747-1567.1992.tb00702.x.

[85] E.S. Bernard, Flexural Behaviour of Cold-Formed Profiled Steel Decking, 1993.

[86] Y.B. Kwon, Post-buckling Behaviour of Thin-Walled Channel Sections, 1992.

[87] C.-C. Weng, Flexural buckling of cold-formed steel columns, Diss. Abstr. Int. 48 (1987) 302.

[88] B. Young, K.J.R. Rasmussen, Compression tests of fixed-ended and pin-ended cold-formed plain channels, Technical Report (University of Sydney School of Civil Engineering) (1995).

[89] B. Young, K.J.R. Rasmussen, Design of lipped channel columns, J. Struct. Eng. 124 (1998) 140–148, doi:10.1061/(ASCE)0733-9445(1998)124:2(140).

[90] B. Young, J. Yan, Finite element analysis and design of fixed-ended plain channel columns, Finite Elem. Anal. Des. 38 (2002) 549–566, doi:10.1016/S0168-874X(01)00085-3.

[91] B. Young, J. Yan, Channel columns undergoing local, distortional, and overall buckling, J. Struct. Eng. 128 (2002) 728–736, doi:10.1061/(ASCE)0733-9445(2002)128:6(728).

[92] E. Ellobody, B. Young, Behavior of cold-formed steel plain angle columns, J. Struct. Eng. 131 (2005) 457–466, doi:10.1061/(ASCE)0733-9445(2005)131:3(457).

[93] B. Young, E. Ellobody, Buckling analysis of cold-formed steel lipped angle columns, J. Struct. Eng. 131 (2005) 1570–1579, doi:10.1061/(ASCE)0733-9445(2005)131:10(1570).

[94] B. Somodi, B. Kövesdi, Residual stress measurements on cold-formed HSS hollow section columns, J. Constr. Steel Res. 128 (2017) 706–720, doi:10.1016/J.JCSR.2016.10.008.

[95] K.H. Law, L. Gardner, Lateral instability of elliptical hollow section beams, Eng. Struct. 37 (2012) 152–166, doi:10.1016/j.engstruct.2011.12.008.

[96] R.H. Leggatt, D.J. Smith, S.D. Smith, F. Faure, Development and experimental validation of the deep hole method for residual stress measurement, J. Strain Anal. Eng. Des. 31 (1996) 177–186, doi:10.1243/03093247V313177.

[97] A.H. Mahmoudi, S. Hossain, C.E. Truman, D.J. Smith, M.J. Pavier, A new procedure to measure near yield residual stresses using the deep hole drilling technique, Exp. Mech. 49 (2009) 595–604, doi:10.1007/s11340-008-9164-y.

[98] T. Negem, Residual Stress Analysis within Structures Using Incremental Hole Drilling, 2018.

[99] F. Hosseinzadeh, D.J. Smith, C.E. Truman, Through thickness residual stresses in large rolls and sleeves for metal working industry, Mater. Sci. Technol. 25 (2009) 862–873, doi:10.1179/174328408X363335.

[100] M. Barsanti, M. Beghini, C. Santus, A. Benincasa, L. Bertelli, Integral method coefficients and regularization procedure for the ring-core residual stress measurement technique, Adv. Mater. Res., Trans Tech Publ, 2014, pp. 331–336.

[101] P. Šarga, F. Menda, Comparison of ring-core method and hole-drilling method used for determining residual stresses, Am. J. Mech. Eng. 1 (2013) 335–338.

[102] M. Barsanti, M. Beghini, C. Santus, A. Benincasa, L. Bertelli, Integral method coefficients for the ring-core technique to evaluate non-uniform residual stresses, J. Strain Anal. Eng. Des. 53 (2018) 210–224, doi:10.1177/0309324718760438.

[103] F. Menda, F. Trebuňa, P. Šarga, Determination of the necessary geometric parameters of the specimen in ring-core method, Appl. Mech. Mater., Trans Tech Publ, 2014, pp. 90–95.

[104] N. Sabaté, D. Vogel, A. Gollhardt, J. Keller, C. Cané, I. Gràcia, J.R. Morante, B. Michel, Residual stress measurement on a MEMS structure with high-spatial resolution, J. Microelectromechanical Syst. 16 (2007) 365–372, doi:10.1109/JMEMS.2006.879701.

[105] A.J.G. Lunt, A.M. Korsunsky, A review of micro-scale focused ion beam milling and digital image correlation analysis for residual stress evaluation and error estimation, Surf. Coating. Technol. 283 (2015), doi:10.1016/j.surfcoat.2015.10.049.

[106] X. Song, K.B. Yeap, J. Zhu, J. Belnoue, M. Sebastiani, E. Bemporad, K.Y. Zeng, A.M. Korsunsky, Residual stress measurement in thin films using the semi-destructive ring-core drilling method using Focused Ion Beam, Procedia Eng., Elsevier Ltd, 2011, pp. 2190–2195, doi:10.1016/j.proeng.2011.04.362.

[107] A.M. Korsunsky, M. Sebastiani, E. Bemporad, Residual stress evaluation at the micrometer scale: analysis of thin coatings by FIB milling and digital image correlation, Surf. Coating. Technol. 205 (2010) 2393–2403, doi:10.1016/j.surfcoat.2010.09.033.

[108] ASTM E837 - 13a, Standard Test Method for Determining Residual Stresses by the Hole-Drilling Strain-Gage Method, 2013. https://www.astm.org/Standards/E837.

[109] G.S. Schajer, Measurement of non-uniform residual stresses using the hole-drilling method. Part II—practical application of the integral method, J. Eng. Mater. Technol. 110 (1988) 344, doi:10.1115/1.3226060.

[110] J.M. Alegre, A. Díaz, I.I. Cuesta, J.M. Manso, Analysis of the influence of the thickness and the hole radius on the calibration coefficients in the hole-drilling method for the determination of non-uniform residual stresses, Exp. Mech. 59 (2019), doi:10.1007/s11340-018-0433-0.

[111] V.S. Pisarev, V.V. Balalov, V.S. Aistov, M.M. Bondarenko, M.G. Yustus, Reflection hologram interferometry combined with hole drilling technique as an effective tool for residual stresses fields investigation in thin-walled structures, Optic Laser. Eng. 36 (2001) 551–597, doi:10.1016/S0143-8166(01)00065-3.

[112] V.S. Pisarev, M.M. Bondarenko, A.V. Chernov, A.N. Vinogradova, General approach to residual stresses determination in thin-walled structures by combining the hole drilling method and reflection hologram interferometry, Int. J. Mech. Sci. 47 (2005) 1350–1376, doi:10.1016/j.ijmecsci.2005.05.002.

[113] Y. Min, M. Hong, Z. Xi, L. Jian, Determination of residual stress by use of phase shifting moiré interferometry and hole-drilling method, Optic Laser. Eng. 44 (2006) 68–79, doi:10.1016/j.optlaseng.2005.02.006.

[114] J. Ribeiro, J. Monteiro, H. Lopes, M. Vaz, Moiré interferometry assessement of residual stress variation in depth on a shot peened surface, Strain 47 (2011) e542–e550, doi:10.1111/j.1475-1305.2009.00653.x.

[115] G.S. Schajer, M. Steinzig, Full-field calculation of hole drilling residual stresses from electronic speckle pattern interferometry data, Exp. Mech. 45 (2005) 526–532, doi:10.1007/bf02427906.

[116] M. Steinzig, E. Ponslet, Residual stress measurement using the hole drilling method and laser speckle interferometry: part 1, Exp. Tech. 27 (2003) 43–46, doi:10.1111/j.1747-1567.2003.tb00114.x.

[117] L.R. Lothhammer, M.R. Viotti, A. Albertazzi, C.L.N. Veiga, Residual stress measurements in steel pipes using DSPI and the hole-drilling technique, Int. J. Pres. Ves. Pip. 152 (2017) 46–55, doi:10.1016/j.ijpvp.2017.05.008.

[118] M.J. McGinnis, S. Pessiki, H. Turker, Application of three-dimensional digital image correlation to the core-drilling method, Exp. Mech. 45 (2005) 359–367, doi:10.1007/bf02428166.

[119] J.D. Lord, D. Penn, P. Whitehead, The application of digital image correlation for measuring residual stress by incremental hole drilling, Appl. Mech. Mater., Trans Tech Publ, 2008, pp. 65–73.

[120] G.S. Schajer, Advances in Hole-drilling residual stress measurements, Exp. Mech. 50 (2010) 159–168, doi:10.1007/s11340-009-9228-7.

[121] H. Wern, A new approach to triaxial residual stress evaluation by the hole drilling method, Strain 33 (1997) 121–126, doi:10.1111/j.1475-1305.1997.tb01059.x.

[122] G.S. Schajer, Hole-drilling residual stress measurements at 75: origins, advances, opportunities, Exp. Mech. 50 (2010) 245–253.

[123] D. von Mirbach, Four-point bending tests to study the so-called plasticity effect on the residual stress results determined by the hole-drilling and ring-core methods, Adv. Mater. Res., Trans Tech Publ, 2014, pp. 319–324.

[124] H. Heidary, M. Sadri, N.Z. Karimi, C. Fragassa, Numerical study of plasticity effects in uniform residual stresses measurement by ring-core technique, J. Serb. Soc. Comput. Mech. 11 (2017) 17–26.

[125] Z.H. Yan, S.Y. Wu, P. Yi, L.Y. Pin, C.Y. Jun, On the correction of plasticity effect at the hole edge when using the centre hole method for measuring high welding residual stress, Strain 32 (1996) 125–130, doi:10.1111/j.1475-1305.1996.tb01017.x.

[126] M. Ermini, Plasticity effects in residual stress measurement by the hole drilling method, Strain 36 (2000) 55–59, doi:10.1111/j.1475-1305.2000.tb01174.x.

[127] M. Beghini, L. Bertini, P. Raffaelli, Numerical analysis of plasticity effects in the hole-drilling residual stress measurement, J. Test. Eval. 22 (1994) 522–529.

[128] M. Beghini, L. Bertini, P. Raffaelli, An account of plasticity in the hole-drilling method of residual stress measurement, J. Strain Anal. Eng. Des. 30 (1995) 227–233, doi:10.1243/03093247V303227.

[129] M. Beghini, L. Bertini, Recent advances in the hole drilling method for residual stress measurement, J. Mater. Eng. Perform. 7 (1998) 163–172, doi:10.1361/105994998770347882.

[130] M. Beghini, L. Bertini, C. Santus, A procedure for evaluating high residual stresses using the blind hole drilling method, including the effect of plasticity, J. Strain Anal. Eng. Des. 45 (2010) 301–318, doi:10.1243/03093247JSA579.

[131] M. Beghini, C. Santus, E. Valentini, A. Benincasa, Experimental verification of the hole drilling plasticity effect correction, Mater. Sci. Forum, Trans Tech Publ, 2011, pp. 151–158.

[132] J.P. Nobre, M. Kornmeier, B. Scholtes, Plasticity effects in the hole-drilling residual stress measurement in peened surfaces, Exp. Mech. 58 (2018) 369–380, doi:10.1007/s11340-017-0352-5.

[133] S. Chupakhin, N. Kashaev, B. Klusemann, N. Huber, Artificial neural network for correction of effects of plasticity in equibiaxial residual stress profiles measured by hole drilling, J. Strain Anal. Eng. Des. 52 (2017) 137–151, doi:10.1177/0309324717696400.

[134] G.S. Schajer, C. Abraham, Residual stress measurements in finite-thickness materials by hole-drilling, Exp. Mech. 54 (2014) 1515–1522, doi:10.1007/s11340-014-9935-6.

[135] G.S. Schajer, Compact calibration data for hole-drilling residual stress measurements in finite-thickness specimens, Exp. Mech. (2020) 1–14, doi:10.1007/s11340-020-00587-4.

[136] J.M. Alegre, A. Díaz, I.I. Cuesta, J.M. Manso, Application of the hole-drilling method for the evaluation of residual stresses near rounded ends, J. Strain Anal. Eng. Des. 54 (2019) 424–430, doi:10.1177/0309324719833227.

[137] S. Schuster, M. Steinzig, J. Gibmeier, Incremental hole drilling for residual stress analysis of thin walled components with regard to plasticity effects, Exp. Mech. 57 (2017) 1457–1467, doi:10.1007/s11340-017-0318-7.

[138] M. De Giorgi, Residual stress evolution in cold-rolled steels, Int. J. Fatig. 33 (2011) 507–512, doi:10.1016/j.ijfatigue.2010.10.006.

[139] M. Beghini, L. Bertini, Analytical expressions of the influence functions for accuracy and versatility improvement in the hole-drilling method, J. Strain Anal. Eng. Des. 35 (2000) 125–135, doi:10.1243/0309324001514071.

[140] M. Beghini, L. Bertini, L.F. Mori, Evaluating non-uniform residual stress by the hole-drilling method with concentric and eccentric holes. Part I. Definition and validation of the influence functions, Strain 46 (2010) 324–336, doi:10.1111/j.1475-1305.2009.00683.x.

[141] M. Beghini, L. Bertini, L.F. Mori, Evaluating non-uniform residual stress by the hole-drilling method with concentric and eccentric holes. Part II: application of the influence functions to the inverse problem, Strain 46 (2010) 337–346, doi:10.1111/j.1475-1305.2009.00684.x.

[142] L. Tong, G. Hou, Y. Chen, F. Zhou, K. Shen, A. Yang, Experimental investigation on longitudinal residual stresses for cold-formed thick-walled square hollow sections, J. Constr. Steel Res. 73 (2012) 105–116, doi:10.1016/j.jcsr.2012.02.004.

[143] P. Grant, Evaluation of Residual Stress Measurement Uncertainties Using X-Ray Diffraction and Hole Drilling via a UK Intercomparison Exercise, 2002.

[144] M. Jandera, L. Gardner, J. Machacek, Residual stresses in cold-rolled stainless steel hollow sections, J. Constr. Steel Res. 64 (2008) 1255–1263, doi:10.1016/J.JCSR.2008.07.022.

[145] S.H. Li, G. Zeng, Y.F. Ma, Y.J. Guo, X.M. Lai, Residual stresses in roll-formed square hollow sections, Thin-Walled Struct. 47 (2009) 505–513, doi:10.1016/j.tws.2008.10.015.

[146] F. Wang, J. Yang, I. Azim, L. Bai, Y. Ma, Experimental and numerical evaluations of the distribution and effect of roll-forming residual stress on CFS sigma beams, J. Constr. Steel Res. 167 (2020) 105978, doi:10.1016/j.jcsr.2020.105978.

[147] Y. Nakayama, T. Takaai, S. Kimura, Evaluation of surface residual stresses in cold-rolled 5083 aluminum alloy by X-ray method, Mater. Trans., JIM 34 (1993) 496–503.

[148] A. Bahadur, B.R. Kumar, S.G. Chowdhury, Evaluation of changes in X-ray elastic constants and residual stress as a function of cold rolling of austenitic steels, Mater. Sci. Technol. 20 (2004) 387–392, doi:10.1179/026708304225012170.

[149] T. Mehner, A. Bauer, S. Härtel, B. Awiszus, T. Lampke, Residual-stress evolution of cold-rolled DC04 steel sheets for different initial stress states, Finite Elem. Anal. Des. 144 (2018) 76–83, doi:10.1016/j.finel.2017.11.006.

[150] S.P. Sagar, B.R. Kumar, G. Dobmann, D.K. Bhattacharya, Magnetic characterization of cold rolled and aged AISI 304 stainless steel, NDT E Int. 38 (2005) 674–681, doi:10.1016/j.ndteint.2005.04.004.

[151] Y.D. Wang, R. Lin Peng, X.L. Wang, R.L. McGreevy, Grain-orientation-dependent residual stress and the effect of annealing in cold-rolled stainless steel, Acta Mater. 50 (2002) 1717–1734, doi:10.1016/S1359-6454(02)00021-6.

[152] L. Pintschovius, V. Hauk, W.K. Krug, Neutron diffraction study of the residual stress state of a cold-rolled steel strip, Mater. Sci. Eng. 92 (1987) 1–12, doi:10.1016/0025-5416(87)90151-0.

[153] S. Harjo, Y. Tomota, M. Ono, Measurements of thermal residual elastic strains in ferrite-austenite Fe-Cr-Ni alloys by neutron and X-ray diffractions, Acta Mater. 47 (1998) 353–362, doi:10.1016/S1359-6454(98)00300-0.

[154] M.T. Hutchings, Introduction to the Characterization of Residual Stress by Neutron Diffraction, CRC press, 2005.

[155] A. Abvabi, Effect of Residual Stresses in Roll Forming Process of Metal Sheets, Deakin University, 2014.

[156] V. García Navas, I. Ferreres, J.A. Marañón, C. Garcia-Rosales, J. Gil Sevillano, Electro-discharge machining (EDM) versus hard turning and grinding-Comparison of residual stresses and surface integrity generated in AISI O1 tool steel, J. Mater. Process. Technol. 195 (2008) 186–194, doi:10.1016/j.jmatprotec.2007.04.131.

[157] ASTM E1558-09(2014), Standard Guide for Electrolytic Polishing of Metallographic Specimens, 2014, doi:10.1520/E1558-09R14.

[158] D. Landolt, Fundamental aspects of electropolishing, Electrochim. Acta 32 (1987) 1–11.

[159] ASTM E3-11 (2017), Standard Guide for Preparation of Metallographic Specimens, 2017, doi:10.1520/E0003-11R17.

[160] M.G. Moore, W.P. Evans, Mathematical correction for stress in removed layers in X-ray diffraction residual stress analysis, SAE Trans. 66 (1958) 340–345. http://www.jstor.org/stable/44554157.

[161] V. Savaria, F. Bridier, P. Bocher, Computational quantification and correction of the errors induced by layer removal for subsurface residual stress measurements, Int. J. Mech. Sci. 64 (2012) 184–195, doi:10.1016/j.ijmecsci.2012.07.003.

[162] B. Nagarajan, D. Kumar, Z. Fan, S. Castagne, Effect of deep cold rolling on mechanical properties and microstructure of nickel-based superalloys, Mater. Sci. Eng. 728 (2018) 196–207, doi:10.1016/j.msea.2018.05.005.

[163] M.F. de Campos, M.J. Sablik, F.J.G. Landgraf, T.K. Hirsch, R. Machado, R. Magnabosco, C.J. Gutierrez, A. Bandyopadhyay, Effect of rolling on the residual stresses and magnetic properties of a 0.5% Si electrical steel, J. Magn. Magn Mater. 320 (2008) e377–e380, doi:10.1016/j.jmmm.2008.02.104.

[164] B. Schafer, T. Pekoz, Direct strength prediction of cold-formed steel members using numerical elastic buckling solutions, International Specialty Conference on Cold-Formed Steel Structures 4 (1998) 69–76.

[165] C. Yu, B.W. Schafer, Distortional buckling tests on cold-formed steel beams, J. Struct. Eng. 132 (2006) 515–528, doi:10.1061/(ASCE)0733-9445(2006)132:4(515).

[166] C. Yu, W. Yan, Effective Width Method for determining distortional buckling strength of cold-formed steel flexural C and Z sections, Thin-Walled Struct. 49 (2011) 233–238, doi:10.1016/j.tws.2010.11.006.

[167] B.W. Schafer, Review: the Direct Strength Method of cold-formed steel member design, J. Constr. Steel Res. 64 (2008) 766–778, doi:10.1016/j.jcsr.2008.01.022.

[168] C.D. Moen, Direct Strength Design of Cold-Formed Steel Members with Perforations, 2008.

[169] C.D. Moen, B.W. Schafer, Elastic buckling of cold-formed steel columns and beams with holes, Eng. Struct. 31 (2009) 2812–2824, doi:10.1016/j.engstruct.2009.07.007.

[170] J. Bonada, M.M. Pastor, F. Roure, M. Casafont, Influence of the cold work effects in perforated rack columns under pure compression load, Eng. Struct. 97 (2015) 130–139, doi:10.1016/j.engstruct.2015.04.011.

[171] M. Lindgren, Experimental and Computational Investigation of the Roll Forming Process, 2009.

[172] D. Bhattacharyya, P.D. Smith, C.H. Yee, I.F. Collins, The prediction of deformation length in cold roll-forming, J. Mech. Work. Technol. 9 (1984) 181–191, doi:10.1016/0378-3804(84)90004-4.

[173] Q. V Bui, J.P. Ponthot, Numerical simulation of cold roll-forming processes, J. Mater. Process. Technol. 202 (2008) 275–282, doi:10.1016/j.jmatprotec.2007.08.073.

[174] M. Kiuchi, ANALYTICAL STUDY ON COLC-ROLL-FORMING PROCESS, 1973.

[175] M. Kiuchi, T. Koudabashi, Automated design system of optimal roll profiles for cold roll forming, 3 Rd Int. Conf. Rotary Metalwork. Process., 3, 1984, pp. 423–436.

[176] S.M. Panton, D.A. Milner, Computer-Aided design of form-rolls, Adv. Manuf. Technol., Springer US, 1986, pp. 71–78, doi:10.1007/978-1-4757-1355-8_10.

[177] N. Duggal, M.A. Ahmetoglu, G.L. Kinzel, T. Altan, Computer aided simulation of cold roll forming - a computer program for simple section profiles, J. Mater. Process. Technol. 59 (1996) 41–48, doi:10.1016/0924-0136(96)02285-6.

[178] G. Nefussi, P. Gilormini, A simplified method for the simulation of cold-roll forming, Int. J. Mech. Sci. 35 (1993) 867–878, doi:10.1016/0020-7403(93)90045-V.

[179] C. Liu, Modelling of cold roll forming of steel strip, Mater. Sci. Technol. 17 (2001) 415–418, doi:10.1179/026708301101510140.

[180] data M.S.M.S. GmbH, COPRA RF 2011 User Manual. H2-H3. Deformation Technology (Simulation) & Flower Technology, 2011.

[181] C.J. Su, L.Y. Yang, S.M. Lou, G.H. Cao, F.R. Yuan, Q. Wang, Optimized bending angle distribution function of contour plate roll forming, Int. J. Adv. Manuf. Technol. 97 (2018) 1787–1799, doi:10.1007/s00170-018-2053-3.

[182] C.J. Su, L.Y. Yang, S.M. Lou, Q. Wang, R. Wang, Research on roll forming process based on five-boundary condition forming angle distribution function, Int. J. Adv. Manuf. Technol. 102 (2019) 3767–3779, doi:10.1007/s00170-019-03377-y.

[183] Z.T. Zhang, S.J. Hu, Stress and residual stress distributions in plane strain bending, Int. J. Mech. Sci. 40 (1998) 533–543, doi:10.1016/s0020-7403(97)00075-1.

[184] J. Rondal, Residual stresses in cold-rolled profiles, Construct. Build. Mater. 1 (1987) 150–164, doi:10.1016/0950-0618(87)90016-X.

[185] W.M. Quach, J.G. Teng, K.F. Chung, Finite element predictions of residual stresses in press-braked thin-walled steel sections, Eng. Struct. 28 (2006) 1609–1619, doi:10.1016/J.ENGSTRUCT.2006.02.013.

[186] C. Wang, G. Kinzel, T. Altan, Mathematical modeling of plane-strain bending of sheet and plate, J. Mater. Process. Technol. 39 (1993) 279–304, doi:10.1016/0924-0136(93)90164-2.

[187] D.K. Leu, A simplified approach for evaluating bendability and springback in plastic bending of anisotropic sheet metals, J. Mater. Process. Technol. 66 (1997) 9–17, doi:10.1016/S0924-0136(96)02453-3.

[188] G. Huang, L. Wang, H. Zhang, Y. Wang, Z. Shi, F. Pan, Evolution of neutral layer and microstructure of AZ31B magnesium alloy sheet during bending, Mater. Lett. 98 (2013) 47–50, doi:10.1016/j.matlet.2013.02.055.

[189] K. Dilip Kumar, K.K. Appukuttan, V.L. Neelakantha, P.S. Naik, Experimental determination of spring back and thinning effect of aluminum sheet metal during L-bending operation, Mater. Des. 56 (2014) 613–619, doi:10.1016/j.matdes.2013.11.047.

[190] X. li Liu, J. guo Cao, X. ting Chai, Z. lei He, J. Liu, R. guo Zhao, Experimental and numerical prediction of the local thickness reduction defect of complex cross-sectional steel in cold roll forming, Int. J. Adv. Manuf. Technol. 95 (2018) 1837–1848, doi:10.1007/s00170-017-1279-9.

[191] K. Hyunok, N. Nargundkar, T. Altan, Prediction of bend allowance and springback in air bending, J. Manuf. Sci. Eng. Trans. ASME. 129 (2007) 342–351, doi:10.1115/1.2673527.

[192] S.L. Zang, C. Guo, S. Thuillier, M.G. Lee, A model of one-surface cyclic plasticity and its application to springback prediction, Int. J. Mech. Sci. 53 (2011) 425–435, doi:10.1016/j.ijmecsci.2011.03.005.

[193] X. Yang, C. Choi, N.K. Sever, T. Altan, Prediction of springback in air-bending of Advanced High Strength steel (DP780) considering Youngs modulus variation and with a piecewise hardening function, Int. J. Mech. Sci. 105 (2016) 266–272, doi:10.1016/j.ijmecsci.2015.11.028.

[194] T.X. Yu, W. Johnson, Influence of axial force on the elastic-plastic bending and springback of a beam, J. Mech. Work. Technol. 6 (1982) 5–21, doi:10.1016/0378-3804(82)90016-X.

[195] R.H. Wagoner, Sheet springback, Contin. Scale Simul. Eng. Mater., Wiley-VCH Verlag GmbH & Co. KGaA, Weinheim, FRG, 2005, pp. 777–794, doi:10.1002/3527603786.ch42.

[196] R.H. Wagoner, J.F. Wang, M. Li, Springback, Metalwork. Sheet Form 14B (2006) 0, doi:10.31399/asm.hb.v14b.a0005131.

[197] R.H. Wagoner, H. Lim, M.G. Lee, in: Int J. Plast (Ed.), Advanced Issues in Springback, Elsevier Ltd, 2013, pp. 3–20, doi:10.1016/j.ijplas.2012.08.006.

[198] W.M. Quach, J.G. Teng, K.F. Chung, Residual stresses in press-braked stainless steel sections, II: press-braking operations, J. Constr. Steel Res. 65 (2009) 1816–1826, doi:10.1016/j.jcsr.2009.04.011.

[199] L. Gardner, N. Saari, F. Wang, Comparative experimental study of hot-rolled and cold-formed rectangular hollow sections, Thin-Walled Struct. 48 (2010) 495–507, doi:10.1016/j.tws.2010.02.003.

[200] M. Sun, J.A. Packer, Direct-formed and continuous-formed rectangular hollow sections - comparison of static properties, J. Constr. Steel Res. 92 (2014) 67–78, doi:10.1016/j.jcsr.2013.09.013.

[201] W.M. Quach, C. Cai, Analytical solution for residual stresses in cold-formed stainless steel circular hollow sections due to cold bending, Tubul. Struct. XIII, CRC Press, 2010, pp. 230–237.

[202] C. Cai, Analytical Solutions for Residual Stresses in Cold-Formed Steel Circular Hollow Sections Due to Cold Rolling, Master Thesis, University of Macau, Macau, 2009.

[203] X. Zhang, S. Liu, M. Zhao, S.P. Chiew, Residual stress of cold-formed thick-walled steel rectangular hollow sections, Steel Compos. Struct. 22 (2016) 837–853, doi:10.12989/scs.2016.22.4.837.

[204] A. Mutafi, N. Yidris, M.R. Ishak, R. Zahari, An investigation on longitudinal residual strains distribution of thin-walled press-braked cold formed steel sections using 3D FEM technique, Heliyon 4 (2018) e00937, doi:10.1016/j.heliyon.2018.e00937.

[205] S. Thipprakmas, Finite element analysis of punch height effect on V-bending angle, Mater. Des. 31 (2010) 1593–1598, doi:10.1016/j.matdes.2009.09.019.

[206] S. Thipprakmas, S. Rojananan, Investigation of spring-go phenomenon using finite element method, Mater. Des. 29 (2008) 1526–1532, doi:10.1016/j.matdes.2008.02.002.

[207] D. Rèche, J. Besson, T. Sturel, X. Lemoine, A.F. Gourgues-Lorenzon, Analysis of the air-bending test using finite-element simulation: application to steel sheets, Int. J. Mech. Sci. 57 (2012) 43–53, doi:10.1016/j.ijmecsci.2012.01.014.

[208] S.S. Miranda, M.R. Barbosa, A.D. Santos, J.B. Pacheco, R.L. Amaral, Forming and springback prediction in press brake air bending combining finite element analysis and neural networks, J. Strain Anal. Eng. Des. 53 (2018) 584–601, doi:10.1177/0309324718798222.

[209] Z. Fu, J. Mo, L. Chen, W. Chen, Using genetic algorithm-back propagation neural network prediction and finite-element model simulation to optimize the process of multiple-step incremental air-bending forming of sheet metal, Mater. Des. 31 (2010) 267–277, doi:10.1016/j.matdes.2009.06.019.

[210] T.X. Yu, W. Johnson, The press-brake bending of rigid/linear work-hardening plates, Int. J. Mech. Sci. 23 (1981) 307–318, doi:10.1016/0020-7403(81)90034-5.

[211] M. Brunet, S. Mguil, P. Pol, Modelling of a roll-forming process with a combined 2D and 3D FEM code, J. Mater. Process. Technol. 80– 81 (1998) 213–219, doi:10.1016/S0924-0136(98)00107-1.

[212] P. Groche, C. Mueller, T. Traub, K. Butterweck, Experimental and numerical determination of roll forming loads, Steel Res. Int. 85 (2014) 112–122, doi:10.1002/srin.201300190.

[213] J.-J. Sheu, Simulation and optimization of the cold roll-forming process, AIP Conf. Proc., AIP Publishing, 2004, pp. 452–457, doi:10.1063/1.1766566.

[214] J. Paralikas, K. Salonitis, G. Chryssolouris, Investigation of the effect of roll forming pass design on main redundant deformations on profiles from AHSS, Int. J. Adv. Manuf. Technol. 56 (2011) 475–491, doi:10.1007/s00170-011-3208-7.

[215] R.C. Spoorenberg, H.H. Snijder, J.C.D. Hoenderkamp, Finite element simulations of residual stresses in roller bent wide flange sections, J. Constr. Steel Res. 67 (2011) 39–50, doi:10.1016/j.jcsr.2010.07.004.

[216] J.P. Ponthot, Traitement unifié de la mécanique des milieux continus solides en grandes déformations par la méthode des éléments finis, 1995.

[217] R. Boman, L. Papeleux, Q.V. Bui, J.P. Ponthot, Application of the Arbitrary Lagrangian Eulerian formulation to the numerical simulation of cold roll forming process, J. Mater. Process. Technol. 177 (2006) 621–625, doi:10.1016/j.jmatprotec.2006.04.120.

[218] R. Boman, J.P. Ponthot, Application of the arbitrary Lagrangian eulerian formalism to stationary roll forming simulations, Adv. Mater. Res. 189–193 (2011) 1827–1833, doi:10.4028/www.scientific.net/AMR.189-193.1827.

[219] B. Rossi, H. Degée, R. Boman, Numerical simulation of the roll forming of thin-walled sections and evaluation of corner strength enhancement, Finite Elem. Anal. Des. 72 (2013) 13–20, doi:10.1016/j.finel.2013.04.002.

[220] Y. Crutzen, R. Boman, L. Papeleux, J.P. Ponthot, Lagrangian and arbitrary Lagrangian Eulerian simulations of complex roll-forming processes, Compt. Rendus Mec. 344 (2016) 251–266, doi:10.1016/j.crme.2016.02.005.

[221] M.A. Sheikh, R.R. Palavilayil, An assessment of finite element software for application to the roll-forming process, J. Mater. Process. Technol. 180 (2006) 221–232, doi:10.1016/j.jmatprotec.2006.06.009.

[222] F. Heislitz, H. Livatyali, M.A. Ahmetoglu, G.L. Kinzel, T. Altan, Simulation of roll forming process with the 3-D FEM code PAM-STAMP, J. Mater. Process. Technol. 59 (1996) 59–67, doi:10.1016/0924-0136(96)02287-x.

[223] S. Ján, J. Miroslav, Springback prediction in sheet metal forming processes, J. Technol. Plast. 37 (2012).

[224] M.O. Görtan, D. Vucic, P. Groche, H. Livatyali, Roll forming of branched profiles, J. Mater. Process. Technol. 209 (2009) 5837–5844, doi:10.1016/j.jmatprotec.2009.07.004.

[225] J.H. Wiebenga, M. Weiss, B. Rolfe, A.H. Van Den Boogaard, Product defect compensation by robust optimization of a cold roll forming process, J. Mater. Process. Technol. 213 (2013) 978–986, doi:10.1016/j.jmatprotec.2013.01.006.

[226] M.M. Pastor, J. Bonada, F. Roure, M. Casafont, Residual stresses and initial imperfections in non-linear analysis, Eng. Struct. 46 (2013) 493–507, doi:10.1016/j.engstruct.2012.08.013.

[227] C. Jiao-Jiao, C. Jian-Guo, Z. Qiu-Fang, L. Jiang, Y. Ning, Z. Rong-guo, A novel approach to springback control of high-strength steel in cold roll forming, Int. J. Adv. Manuf. Technol. (2020) 1–12, doi:10.1007/s00170-020-05154-8.

[228] A. Sedlmaier, Press release - roll form and tube mill tooling – COPRA® RF presentation of COPRA® FEA RF – simulation software, Exhib. Tube China 2010, 2010 Shanghai.

[229] Y. Yan, H. Nie, H. Wang, Q. Li, Y. Liu, A novel roll-die forming technology and its FEM simulation, Procedia Eng., Elsevier Ltd, 2017, pp. 1302–1307, doi:10.1016/j.proeng.2017.10.887.

[230] M.S. Tehrani, P. Hartley, H.M. Naeini, H. Khademizadeh, Localised edge buckling in cold roll-forming of symmetric channel section, Thin-Walled Struct. 44 (2006) 184–196, doi:10.1016/j.tws.2006.01.008.

[231] W. Kang, Y. Zhao, W. Yu, S. Wang, Y. Ma, P. Yan, Numerical simulation and parameters analysis for roll forming of martensitic steel MS980, Procedia Eng., Elsevier Ltd, 2014, pp. 251–256, doi:10.1016/j.proeng.2014.09.159.

[232] R. Safdarian, H. Moslemi Naeini, The effects of forming parameters on the cold roll forming of channel section, Thin-Walled Struct. 92 (2015) 130–136, doi:10.1016/j.tws.2015.03.002.

[233] M. Muller, S.M. Barrans, L. Blunt, Predicting plastic deformation and work hardening during V-band formation, J. Mater. Process. Technol. 211 (2011) 627–636, doi:10.1016/j.jmatprotec.2010.11.020.

[234] Y. Crutzen, R. Boman, L. Papeleux, J.P. Ponthot, Continuous roll forming including in-line welding and post-cut within an ALE formalism, Finite Elem. Anal. Des. 143 (2018) 11–31, doi:10.1016/j.finel.2018.01.005.

[235] Y. Yao, W.M. Quach, B. Young, Finite element-based method for residual stresses and plastic strains in cold-formed steel hollow sections, Eng. Struct. 188 (2019) 24–42, doi:10.1016/j.engstruct.2019.03.010.

[236] Y. Yao, W.M. Quach, B. Young, Simplified models for residual stresses and equivalent plastic strains in cold-formed steel elliptical hollow sections, Thin-Walled Struct. 154 (2020) 106835, doi:10.1016/j.tws.2020.106835.

[237] Y. Yao, W.M. Quach, B. Young, Cross-section behavior of cold-formed steel elliptical hollow sections – a numerical study, Eng. Struct. 201 (2019) 109797, doi:10.1016/j.engstruct.2019.109797.
[238] S. Hong, S. Lee, N. Kim, A parametric study on forming length in roll forming, J. Mater. Process. Technol., Elsevier, 2001, pp. 774–778, doi:10.1016/S0924-0136(01)00711-7.
[239] A. Matuszak, Factors influencing friction in steel sheet forming, J. Mater. Process. Technol. 106 (2000) 250–253, doi:10.1016/S0924-0136(00)00625-7.
[240] M. Weiss, B. Abeyrathna, B. Rolfe, A. Abee, H. Wolfkamp, Effect of coil set on shape defects in roll forming steel strip, J. Manuf. Process. 25 (2017) 8–15, doi:10.1016/j.jmapro.2016.10.005.
[241] K. Louaisil, M. Dubar, R. Deltombe, A. Dubois, L. Dubar, Analysis of interface temperature, forward slip and lubricant influence on friction and wear in cold rolling, Wear 266 (2009) 119–128, doi:10.1016/j.wear.2008.06.003.
[242] V.B. Nguyen, C.J. Wang, D.J. Mynors, M.A. Castellucci, M.A. English, Finite element simulation on mechanical and structural properties of cold-formed dimpled steel, Thin-Walled Struct. 64 (2013) 13–22, doi:10.1016/j.tws.2012.11.002.
[243] V.B. Nguyen, C.J. Wang, D.J. Mynors, M.A. English, M.A. Castellucci, Dimpling process in cold roll metal forming by finite element modelling and experimental validation, J. Manuf. Process. 16 (2014) 363–372, doi:10.1016/j.jmapro.2014.03.001.
[244] A. Abvabi, B. Rolfe, P. Hodgson, M. Weiss, Development of an inverse routine to predict residual stresses in the material based on a bending test, Key Eng. Mater. 554–557 (2013) 949–956, doi:10.4028/www.scientific.net/KEM.554-557.949.
[245] A. Abvabi, B. Rolfe, P.D. Hodgson, M. Weiss, The influence of residual stress on a roll forming process, Int. J. Mech. Sci. 101–102 (2015) 124–136, doi:10.1016/j.ijmecsci.2015.08.004.
[246] S. Narayanan, M. Mahendran, Ultimate capacity of innovative cold-formed steel columns, J. Constr. Steel Res. 59 (2003) 489–508, doi:10.1016/S0143-974X(02)00039-1.
[247] W.M. Quach, J.G. Teng, K.F. Chung, Effect of the manufacturing process on the behaviour of press-braked thin-walled steel columns, Eng. Struct. 32 (2010) 3501–3515, doi:10.1016/j.engstruct.2010.07.019.